CHATTER MODELLING FOR BALL END MICRO MILLING

A Project Report Submitted

in Partial Fulfilment of the Requirements for

the Degree of

Master of Technology

by

Sumit Pal

Roll No.: 224103223

under the guidance of

Dr. R.K. Mittal

DEPARTMENT OF MECHANICAL ENGINEERING

INDIAN INSTITUTE OF TECHNOLOGY GUWAHATI

June 2024

Certificate

This is to certify that the project report entitled "**Chatter Modelling for Ball End Micro Milling**" being submitted to the Indian Institute of Technology Guwahati, India, by Mr. Sumit Pal (Roll No. 224103223) for the fulfilment of the requirement for the degree of Master of Technology is a record of bonafide research work carried out by him under my supervision and he fulfils the requirement of the regulations of the same. The results embodied in this report have not been submitted to any other University or Institute for the award of any degree.

Dr. R.K. Mittal
Assistant Professor
Department of Mechanical Engineering
Indian Institute of Technology Guwahati

Declaration

I **Sumit Pal**, declare that the work contained in this thesis report is composed of my thoughts and ideas. The ideas and materials used from the sources in this book have been appropriately credited in the detailed references. It is to fairly declare that I followed all academic honesty and integrity principles provided by the institute in writing the report. The work has not been submitted to any other institution or university for the award of any degree.

June 06, 2024

Sumit Pal

Roll Number-224103223

Department of Mechanical Engineering

Indian Institute of Technology Guwahati

Acknowledgement

I would like to express my deepest gratitude to Dr. Rinku Kumar Mittal, my supervisor and Assistant Professor in the Department of Mechanical Engineering at IIT Guwahati, India. His constant warmth, motivation, and support have been invaluable throughout the entire journey of my project. His profound expertise in chatter has greatly shaped the direction and scope of this work. The systematic approach he employs in his research has left a significant mark on my own methodologies. I am immensely thankful for the time, insightful guidance, and effort he has dedicated to mentoring me. The knowledge and skills I have gained under his supervision are immeasurable, and I will forever be grateful for his contributions. His constant help in reviewing and improving this thesis has been essential. Without his support, this project would not have happened.

I would like to extend my sincere thanks to Professor K. S. R. Krishna Murthy, Head of the Department of Mechanical Engineering, for providing me with access to the department's research facilities. I am also deeply grateful to the entire faculty, as well as the technical and non-technical staff, for their wholehearted cooperation and support throughout the course of my work. I am also grateful for the friendship and help from my fellow research scholars in the Department of Mechanical Engineering at IIT Guwahati.

I am deeply thankful to my parents for their endless love, generous sacrifices, and constant support during these challenging times. Their guidance and blessings have been crucial in helping me get to this point in my life. I also want to acknowledge the invaluable support of my close friends and colleagues, especially Mr. Abhishek Punia, Mr. Debottam Bhowmik, Mr. Parvez Mushraf, Mr. Ashish Kumar Verma and Mr. Rohit Kumar. Their encouragement and help have been key to achieving this goal.

Finally, I want to express my gratitude to God for helping me overcome all the challenges. I have sensed your guidance every day. Thank you, God.

Mr. Sumit Pal
Department of Mechanical Engineering
Institute of Technology Guwahati

Abstract

Ball end milling is a widely utilized machining process in modern manufacturing, renowned for its versatility in shaping complex surfaces and achieving high precision. However, this process often encounters the adverse effects of tool chatter, which can deteriorate surface quality, shorten tool lifespan, and decrease machining efficiency. Consequently, comprehending and effectively managing chatter during ball end milling holds paramount importance for the manufacturing industry.

This research examines the mechanics and dynamics of cutting with a unique helical ball end cutter. It addresses a variety of factors that influence chatter, including tool geometry, cutting parameters, and machine dynamics. The purpose is to improve the performance and stability of the machining process by creating a computational model that takes these parameters into account. In order to optimise the machining process in terms of productivity, tool life, and surface smoothness, our study offers a greater understanding of the dynamic behaviour of ball end milling.

In this study, chatter and non-chatter zones in high-speed ball end milling were identified utilising the modified zeroth-order approximation (ZOA) method in combination with dynamic force modelling to generate a stability lobe diagram (SLD). From observations it was found the influence of feed rate and depth of cut on cutting forces was systematically investigated. The results showed that both parameters significantly affect the cutting forces, with higher feed rates and greater depths of cut leading to increased forces. The SLD effectively mapped the stable and unstable regions for different combinations of spindle speed and depth of cut. These results should help the process planners in designing tools and in selecting optimum cutting conditions prior to each operation to increase the productivity.

Keywords: Chatter Modelling, Force Modelling, Ball End Milling, Dynamic Analysis.

Contents

Nomenclature

z	Axial depth of cut
h	Uncut chip thickness
s_t	Feed per tooth
ϕ	Radial immersion angle
k	Axial immersion angle
β	Helix angle
R_0	Ball radius
N	Number of flutes / teeth
n	Spindle speed in rpm
dz	Differential height in axial direction
ds	Differential cutting edge length
db	Differential cutting edge width
dF_{tj}	Differential cutting force in tangential direction for tooth j
dF_{rj}	Differential cutting force in radial direction for tooth j
dF_{aj}	Differential cutting force in axial direction for tooth j
K_{tc}	Tangential cutting force coefficients
K_{rc}	Radial cutting force coefficients
K_{ac}	Axial cutting force coefficients
K_{te}	Tangential edge force coefficients
K_{re}	Radial edge force coefficients
K_{ae}	Axial edge force coefficients
ψ	Lag angle
dF_x	Differential cutting force in x direction
dF_y	Differential cutting force in y direction
dF_z	Differential cutting force in z direction
ϕ_p	Cutter pitch angle
ϕ_{st}	Cutting start angle
ϕ_{ex}	Cutting end angle

List of Figures

List of Tables

CHAPTER 1

INTRODUCTION

1.1 Micro Milling

Metal cutting involves removing material from a workpiece with a cutting tool to achieve a desired object. In recent decades, there has been a surge in demand for high-accuracy small and micro components in industries such as aerospace, medical, automotive, electronics, telecommunications, and optics. As demand for highly precise micro-components grows, researchers and institutions are shifting their focus from macro-manufacturing to micro-manufacturing. Micro-manufacturing procedures include micro milling, micro-EDM, micro-grooving, micro drilling, lithography, laser beam machining, and silicon etching to manufacture miniature 2-D and 3-D features. In contrast, micro milling is one of the most important and reliable micro manufacturing solutions for most miniaturised products. Micro milling produces complex 3-D features ranging from a few millimetres to tens of micrometres in materials such as metallic alloys, polymers, ceramics, and composites [1]. Micro milling can produce miniaturised components and goods, including motors/turbines, satellites, biomedical implants, surgical equipment, robotics, and molds/dies [2]. Micro milling improves conventional micromachining technologies in terms of feature complexity and material processing capabilities. This is because micro milling cutters have well-defined cutting edges (helical end mill, ball end mill, bull nose mill etc.) that can achieve high machined surface integrity and dimensional/geometrical accuracy. The micro-end mills have cutting edge radii ranging from 1 to 500 μm [3]. Figure 1.1 depicts a typical 400 μm micro-end mill built of tungsten carbide.

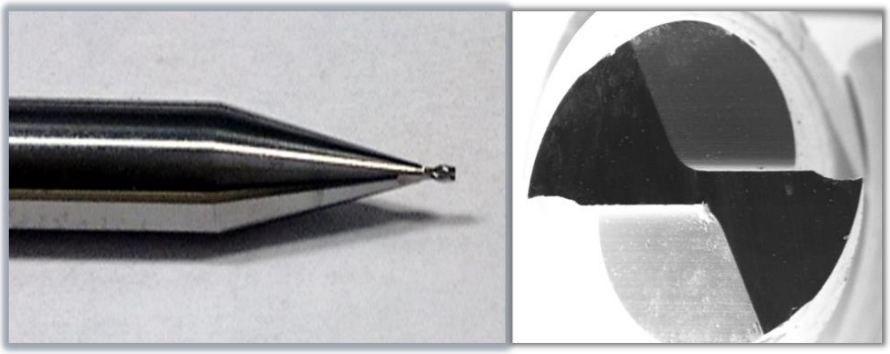

Fig. 1.1 Micro end mill of diameter 400 μm

The goal of precision and efficiency in modern manufacturing has resulted in ever-increasing demands on machining operations, particularly for complicated and curved surfaces. Ball end milling, a versatile and widely used material removal process, is essential in the production of complicated three-dimensional components in industries ranging from aerospace to medical equipment. The technique's versatility with a wide range of materials, including metals, polymers, and composites, has made it a vital tool for creating finely shaped components [4]. As end mill diameters diminish to a few micro metres, micro milling presents unique challenges compared to traditional milling. The challenges of micro milling due to scaling down will be described in the next part.

1.2 Challenges in Micro Milling Processes

Micro-fabrication raises a number of important challenges that need for a shift in perspective away from macro-processes. The main cause of these problems is the diminishing of the elements, tools, and processes. Tool detection and unequal cutting force distribution along the cutting edges are the main problems in micro milling. The tool used to manufacture micro-scale features can have a diameter as small as a few tens of microns. When a tool's diameter is decreased, its flexural stiffness is significantly reduced (by orders of magnitudes compared to macro-tools), which can result in catastrophic tool failure even at relatively low cutting forces. The application of high spindle rotational speeds during micromachining is one method to address this problem. In order to decrease the chip load and hence the forces acting on the cutting edges, high spindle speeds are used. On the other hand, rapid speed creates new difficulties for dynamic stability. When high rotational speeds are combined with low flexural stiffness, high-speed micro milling can lead to dynamic instability. The cutting forces' dynamic variation is the cause of the dynamic instability. Three main factors might cause the dynamic

fluctuation in cutting forces during high-speed micro milling: the material, the machine-tool system, and process mechanics [5], as illustrated in Fig. 1.2.

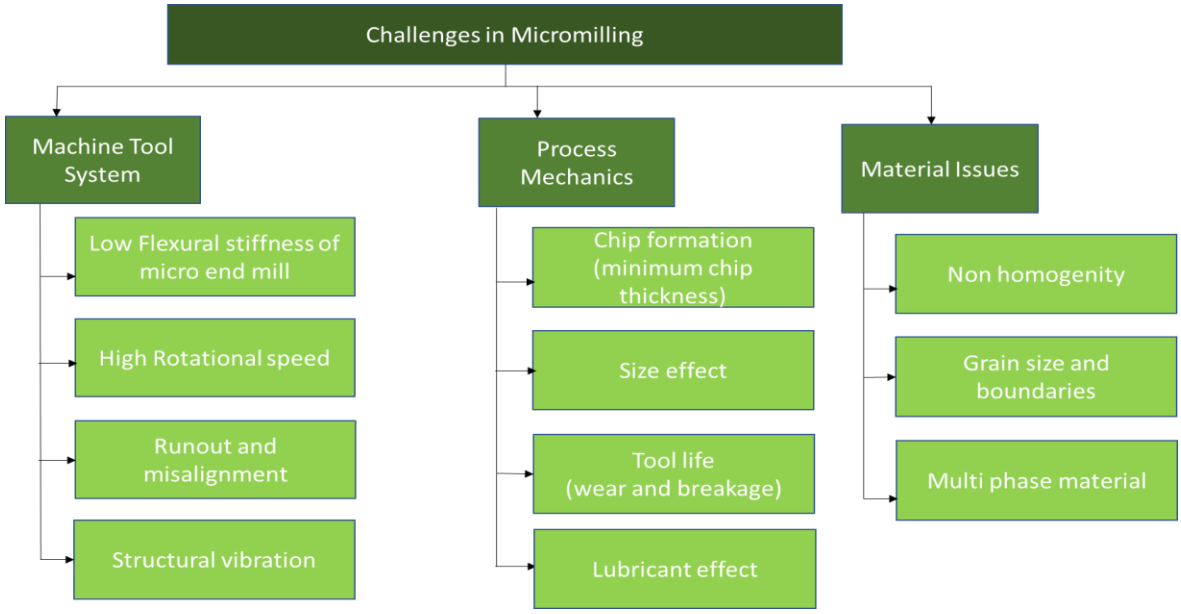

Fig. 1.2 Challenges in micro milling

Machine tool structure related challenges as; (i) Low stiffness of the micro tool due to their size in microscale. Even small force change will damage the tool as stiffness is subjected to force variations. (ii) High rotational speed increases temperature cutting zone (due to the friction between the tool and the workpiece material) which affect the surface integrity and tool because of thermal damage as residual stress, changes in microstructure. (iii) Runout (deviation of the tool from its axis of rotation) and misalignment (axes of the machining tool, workpiece, or machine components are not properly aligned.) will change the cutting force which leads to variations in material removal rates, fluctuations in chip formation and affects the surface integrity. (iv) Vibration affect the dynamic behavior of machine and results into the bad surface and leaves chatter marks on surface.

Processes mechanics related challenges as; (i) In micromachining, a chip will not be formed if the uncut chip thickness (the thickness of the material being removed by the cutting tool in a single cut) is less than a critical value called minimum chip thickness because the material may deform rather than form into a proper chip. (ii) Size effects issues, as Micro tool have edge radius (intersection of the tool's flank and rake surfaces) in few microns. If feed per tooth is less than to the edge radius then ploughing and rubbing can take place because cutting force will not remove material hence which affect the quality of surface. (iii) Tool wear also affects

the surface integrity as due to tool wear tool's geometry changes, leading to dimensional inaccuracies in the machined part. (iv) Lubrication affect the milling process it changes the cutting force which leads to variations in material removal rates, fluctuations in chip formation in the system and affects the machining process.

Material related challenges as; (i) The non-homogeneity in the workpiece microstructure affect the cutting forces, dynamic response of the tool workpiece system, surface generation and chip formation processes. (ii) The grain sizes of material and boundaries in micro milling process changes material properties as both grain size and tool edge radius is comparable during cutting tool engages with individual grains, which leads to abrasive wear and sometimes the tool's edge radius may not effectively engage with the material's grains, leading to inconsistent chip formation. (iii) Multi phase material as the cutting moves from one phase to another these variations affect the cutting forces, dynamic response of the tool.

1.3 Vibrations in Machining Processes

Machine tool experiences the vibration during machining operations [6]. The metal cutting system, comprising elements like the machine tool, tool holding device, spindle, cutting tool, table and workpiece material. Due to the flexibility of these component system experience vibration. There are three distinct types of mechanical vibrations during metal cutting: free vibrations, forced vibrations, and self-excited vibrations shown in fig. 1.3.

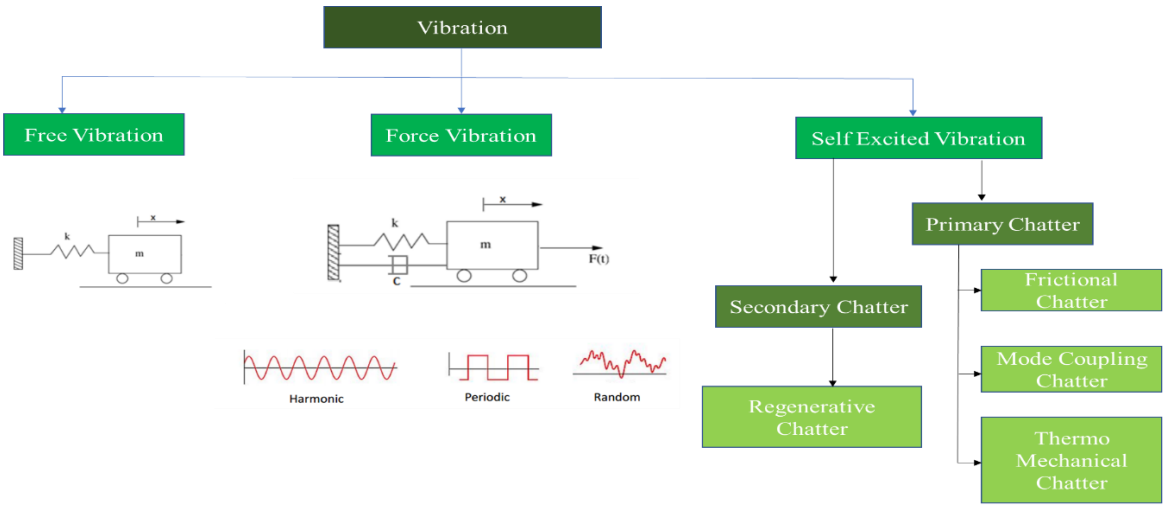

Fig. 1.3 Different types of vibration during machining processes

Free vibrations occur when the system oscillates due to inherent forces resulting from an initial disturbance, without external forces. The system oscillates at natural frequencies determined by its mass and stiffness.

Forced vibrations result from external forces exciting the system. These forces are periodic, harmonic and random in nature. Resonance occurs when the externally induced force frequency matches the system's natural frequency, causing substantial oscillations and potential catastrophic failure.

Self-excited vibration which is called chatter is generated by taking energy from the structure itself. Chatter appears in the system when there is phase difference in current tooth pass and previous tooth pass.

Eliminating or reducing forced and free vibrations can be achieved by locating and regulating their sources, but controlling chatter (self-excited vibrations) is a harder problem to solve.

1.3.1 Self -Excited Vibration or Chatter

Self-excited vibration possesses the inherent characteristic of self-excitation during the machining process. These vibrations establish a closed-loop system involving the cutting process and the dynamics of the machine structure. The dynamic interaction between the cutting tool and workpiece results in periodic internal forces, giving rise to self-induced vibrations. Chatter vibrations derive energy from the cutting process itself, making them self-excited vibrations [7]. Chatter is classified into primary and secondary categories shown in fig. 1.3. Primary chatter stems from the cutting process, while secondary chatter is induced by the regenerative effect, earning it the designation of regenerative chatter. Primary chatter further divides into frictional, thermo-mechanical, and mode-coupling chatter, each distinguished by the specific mechanism of self-excitation.

- Frictional chatter: This arises from the rubbing interaction between the tool's clearance face and the machined surface, leading to vibrations predominantly in the cutting force direction and to a lesser extent in the thrust force direction.[8]
- Thermo-mechanical chatter: It arises from variations in temperature and strain rates within the plastic deformation zone.
- Mode coupling chatter: This phenomenon originates from the interconnection of vibrations occurring in both the cutting and thrust force directions. The coupling of vibrations in one direction induces vibrations in the other direction. As a result,

vibrations are produced concurrently in both the thrust and cutting force directions. The physical factors accountable for the occurrence of mode coupling chatter include fluctuations in chip thickness, friction on the rake and clearance surfaces, oscillations in the shear angle, and the regeneration effect.[9]

- Regenerative chatter: This type of chatter is widely recognized as the most prevalent and is commonly referred to simply as 'chatter' by many researchers. The vibrations originating from the cutting tool result in a wavy surface, as illustrated in Fig. 1.4. This wavy surface leads to fluctuations in chip thickness if the phase difference between the subsequent cut (in milling, caused by the next tooth, and in turning, generated in the next revolution) and the previously cut (wavy) surface is not zero. Consequently, the variable chip thickness gives rise to fluctuating forces on the cutting tool. These variable forces give rise to regenerative chatter, a phenomenon that greatly amplifies vibration and emerges as the most dominant form [10].

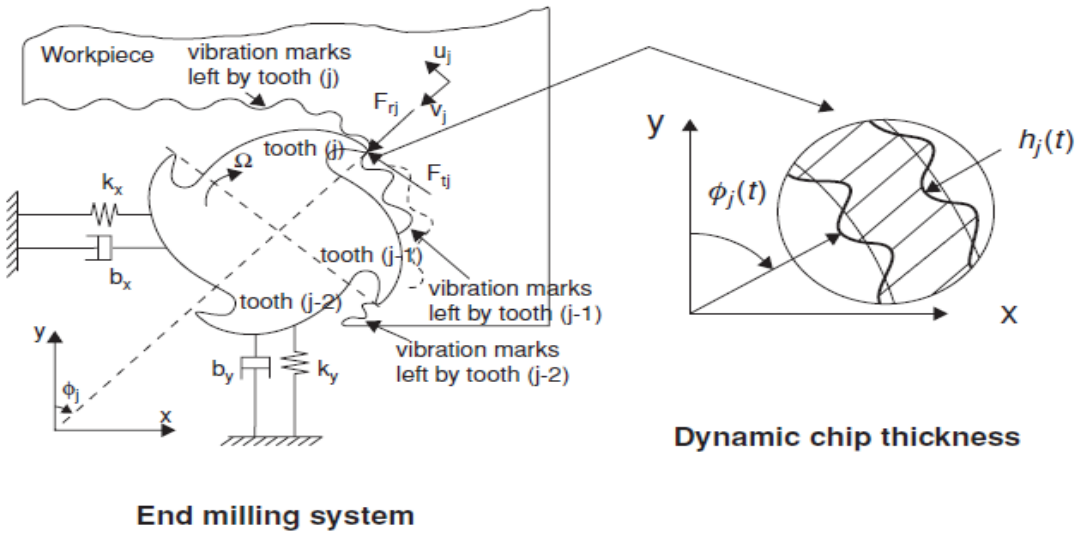

Fig. 1.4 Regeneration of waviness in a milling process and dynamic chip thickness [6]

1.3.2 Detrimental Effects of Chatter in Machining

The adverse outcomes arising from chatter during machining include the following:

- Diminished surface quality.
- Unacceptable precision.
- Accelerated tool wear.
- Damage to the machine tool.
- Reduced material removal rate (MRR).

- Escalated production time and costs.
- Material wastage.
- Energy waste.

1.4 Motivation

Chatter during milling can lead to increased tool wear or breakage, as well as detrimental effects on the surface finish and dimensional accuracy. These outcomes in a manufacturing scenario result in lost revenue from machine damage, re-machining, scrapped products, and downtime. The cost of machining can be greatly reduced by preventing chatter, or by avoiding cutting circumstances that cause chatter vibrations.

This research seeks to deepen the understanding of bifurcations in the milling process and develop a control method for predicting the onset of chatter, specifically identifying the stability boundary of the system. By determining this stability limit, adjustments to milling parameters—such as spindle speed and depth of cut can be made to completely avoid chatter.

1.5 Organization of the Thesis

This thesis is organized into five separate chapters, each containing the following elements:

Chapter 1: Introduction

In this chapter, we provide a concise overview of micro milling processes and ball end micro milling. We also outline the challenges associated with the micro milling processes. In which mechanisms of chatter and its effects on the machined surface is discussed.

Chapter 2: Literature Review

In this chapter, literature review is done on micro milling process and ball end micro milling processes. It includes the mechanistic force modelling, identification of chatter zone. The findings of the literature review are then combined, to find the main research gaps.

Chapter 3: Methodology

In this chapter, develop a computational chatter model for ball end micro milling to calculate the cutting forces and identification of chatter and non-chatter zone. Also, methodology used to develop these models is discussed.

Chapter 4: Results and Discussion

In this chapter, data obtained from the ball end milling test is presented. From the data we identified effects of cutting condition on cutting forces. Also identified chatter and non-chatter zone at given cutting condition.

Chapter 5: Conclusion and Future Scope

In this chapter, based on the outcomes of this ball end micro milling study, we have drawn conclusions and established future directions for this field of work.

CHAPTER 2

LITERATURE REVIEW

The thorough literature analysis of chatter phenomena in the micro milling process and the techniques or approaches to guarantee a stable or chatter-free (stable) machining process are the main topics of the current chapter. The literature review will help in the identification of research gaps based on which future work is proposed. The literature study focuses on two primary areas: high-speed micro milling, and chatter modelling. A flow chart depicting the areas studied in the literature review has been shown in fig. 2.1.

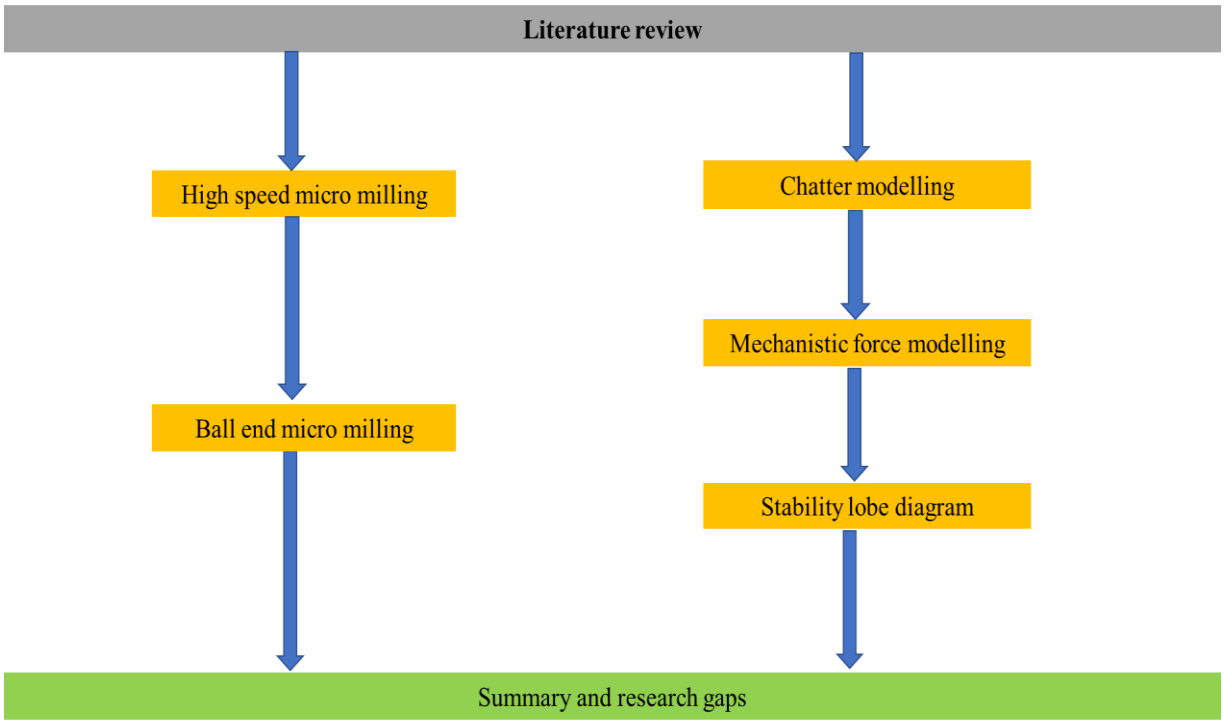

Fig. 2.1 Flow chart for literature review

2.1 Milling Processes

Milling is an important process in the industrial industry since it emphasizes precision and efficiency. This approach entails gradually removing extra material from an original workpiece using a cutting tool to shape, reshape, and improve the surface. The milling cutter, which has numerous cutting edges, rotates while the workpiece is fed in gradually. With each revolution, the cutting edges eliminate chips, leaving a finished surface.

This manufacturing technique is extremely important because of its capacity to manufacture a wide variety of component shapes and sizes with great dimensional accuracy and an outstanding surface finish. Additionally, milling may be readily controlled and mechanized using computer technologies. Understanding the cutting force is critical in many milling operations (Fig 2.2), as it has a direct impact on aspects such as cutter deflection, dimensional tolerance, breakage risk, and processing stability. Understanding the magnitude and variation of cutting force under various cutting situations is critical for optimal process planning in milling operations.

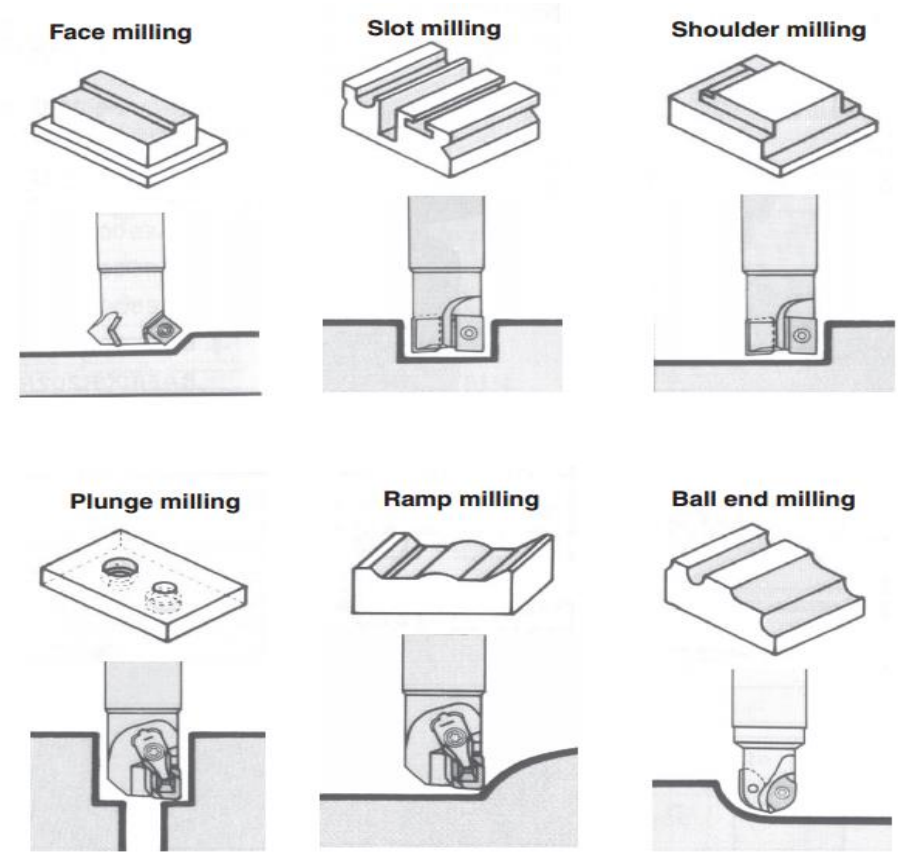

Figure 2.2 Various milling operations [10]

2.1.1 High Speed Micro Milling

Micro-milling is a manufacturing method used to create microscopic components with complex geometry. These components are widely utilised in industries requiring micron-level accuracy, including biomedical, automotive and aerospace. High-speed milling (HSM) is used extensively in today's industrial industry. The primary advantage of high-speed milling is that a significant amount of material may be cut in a short period of time using relatively small tools due to the tool's fast rotational speed [11].

Biermann and Baschin [12] investigated the stability of micro milling processes is affected by the cutting-edge geometry and radius. Due to the small dimensions of the undeformed chip parameter, the cutting edge appears to have a greater influence on chip creation and the regenerative effect than in macro dimensions. This research proposed that a smaller cutting-edge radius leads to instability, whereas a rounder cutting edge leads to stability during machining.

Bandapalli et al. [13] investigated the stability of the system is affected by machining parameters in high-speed micro-end milling. Cutting forces and surface roughness decrease with increased spindle speed and feed rate at a constant depth of cut, while increasing with depth of cut, feed rate, and spindle speed. The cutting depth and feed rate are the parameters that determine the increase in cutting force and surface roughness. The analysis revealed that micro-milling at high spindle speeds, low depth of cut, and low feed rate results in high stability and lower cutting forces.

Ahmadi et al. [14] studied the influence of materials' microstructural properties, including grain size and phase fractions, in micro end milling for stability. To achieve this, the Ti6A14V samples were heat treated to produce two distinct microstructures: fine equiaxed and expanded equiaxed. The study revealed that Micro milling required more cutting force due to smaller grain sizes (α and β) and lower β phase fraction. The sample with expanded equiaxed grains had a higher hardness due to the higher β phase fraction, but had a lower cutting force. because of its poorer ductility.

Mittal et al. [15] investigated the stability of the micro milling processes based on the progressive tool wear. To account for tool wear, cutting force coefficients are modelled based on initial and instantaneous cutting-edge radius (CER) and feed rate per tooth. Tool wear influences stability limitations, including initial CER and feed per tooth. At higher speeds

(90,000-110,000 rpm) progressive tool wear reduces stability limitations by approximately 30%.

2.1.2 Ball End Micro Milling

Ball end milling is a precision machining procedure used in manufacturing impellers, screw propellers, and turbine blades with free form surfaces. However, changing cutting geometry makes it challenging to accomplish high-quality and productive machining. The ball-end mill cutter consists of two parts: a ball and an end mill. The cutting edge's position on a spherical surface results in varying cutting conditions at each point [16].

Altintas and Yucesan [17] presented semi-mechanistic analytical model for the prediction of cutting forces in ball end milling processes. The model is based on the general mechanics of chip generation and tool-workpiece interaction. From study Cutting force distribution and direction are predicted for ball-shaped helical end mills.

Wojciechowski and Twardowski [18] developed a process dynamic model for tool vibration analysis generated during the ball end milling process, including the effect of progressive tool wear. The process dynamics model includes cutting parameters and tool wear width on the flank face. Experiments were conducted on tungsten carbide and cubic boron nitride (CBN) cutters and values of instantaneous cutting forces and vibrations were measured in three directions, along the progression of tool wear. The study found that the tool wear width on the flank face has a significant impact on the vibrations created during the stable milling process and machining with cubic boron nitrite tool stability is more than the sintered carbide tool.

Sonawane and joshi [19] developed analytical models to anticipate cutting tool-workpiece interaction as workpiece inclination changes, resulting in undeformed and distorted chip cross sections. The models calculate the instantaneous shear angle across any cross section of the tool-work interaction on a ball-end cutter during a milling operation. The models demonstrate the evaluation of a chip segment and the mechanics of its production in ball-end milling on an inclined work surface. Study revealed that Chip dimensions, excluding deformed chip thickness, increase with workpiece inclination angle. While the deformed chip thickness decreases due to higher compression during cutting. As higher workpiece inclination angle facilitates the flow of deformed chip across the cutting tool face.

Peng et al. [20] examined how tool inclination angle affects 3D surface topography during micro-ball-end milling. A theoretical model is created to describe the cutting-edge trajectory,

accounting for cutter inclination, flutter, run-out, cutting force, and material plastic deformation. Study revealed that Maintaining a ball-end milling cutter inclination angle of ± 20° results in higher machined stability, while angles more than or less than − 20° result in lower stability.

2.2 Mechanics of Milling

The mechanics of milling can best be understood through an investigation at how chips form during the operation. Martellotti's [21] early thorough study demonstrated that, due to the cutter's combined rotational and linear feeding motions towards the workpiece, the true path of a cutter tooth is an arc of a trochoid rather than a circle, complicating the mathematics in the analysis. However, Martellotti asserted that in most real cutting applications where the cutter radius is significantly bigger than the feed per tooth, the circular tooth path assumption is accurate and the mistake introduced is negligible. As the cutter revolves, the immersion angle (ϕ) varies, and thus the chip thickness changes sinusoidally, as shown by Martellotti:

$$h = s_t \sin\phi \qquad 2.1$$

Where,

h = Instantaneous chip thickness

s_t = Feed per tooth

ϕ = Immersion angle of cutting tool

2.3 Cutting Force Modelling

Micro milling produces more cutting force variation than conventional milling due to the larger feed per unit to tool radius ratios. Micro milling relies significantly on cutting force analysis. Micromachining includes two process mechanisms: ploughing and chip creation. To prevent ploughing during the micro milling process, the uncut chip thickness Should be greater than the minimum chip thickness [22]. To understand the dynamic behaviour of micro milling, first analyse the mechanism of cutting forces.

2.3.1 Mechanistic Force Modelling

Milling tools have several cutting edges at the perimeter and tip, allowing for both end and peripheral cuts. Fig. 2.3 depicts the end milling operation, including cutting forces and chip thickness variations. In addition, the cutting edges of a helical end mill are designed helically having helical flutes which dampens the sharp vibrations in the oscillatory components of the milling force and they are used when depth of cut is large but width of cut is small.

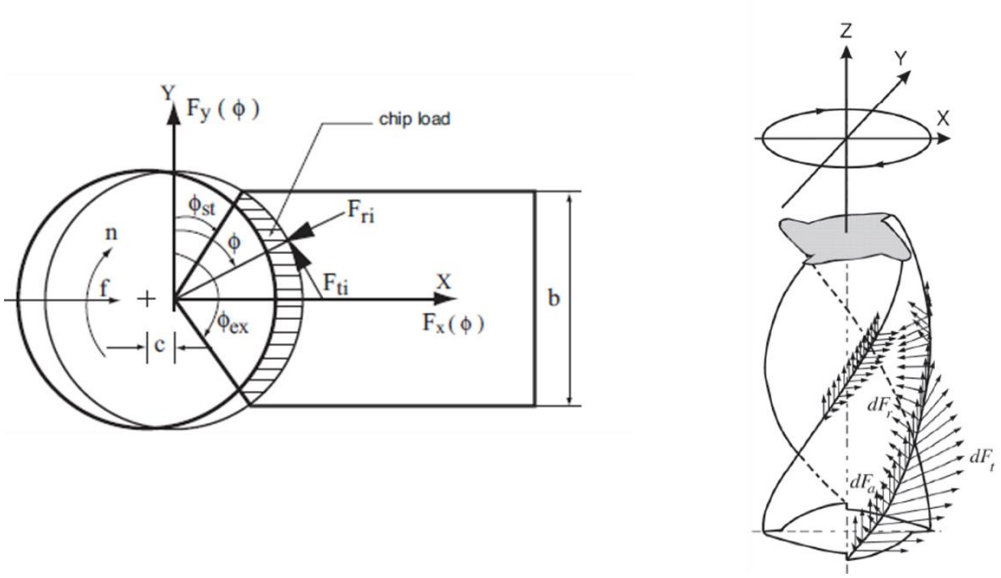

Fig. 2.3 Chip thickness variation and cutting forces in end milling process [6]

A typical end milling cutter with a helix angle β, diameter D, and the number of flutes N depicted in Fig. 2.4 is used for analytical modelling of cutting forces.

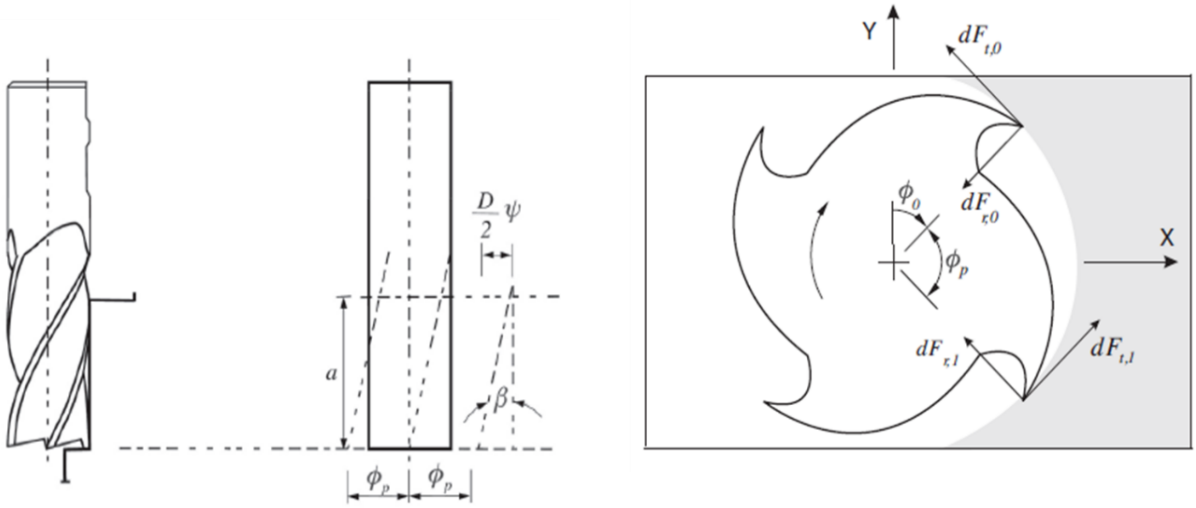

Fig. 2.4 Helical end mill cutter [6]

If bottom end of one tooth is at an immersion angle ϕ then the other tooth's immersion angle at the same instant will be;

$$\phi_j(0) = \phi + j\phi_p \quad ; \quad j = 0,1,2, \ldots\ldots\ldots(N-1) \qquad 2.2$$

Where,

$$\phi_p(\text{tooth spacing angle}) = \frac{2\pi}{N}$$

The immersion angle for flute j (where j = 0,1, 2, …(N-1)) at an axial depth of cut z will depend on lag angle $\psi = k_\beta z$, where $k_\beta = \frac{(2\tan\beta)}{D}$ and is given by,

$$\phi_j(z) = \phi + j\phi_p - k_\beta z \qquad 2.3$$

Tangential ($dF_{t,j}$), radial ($dF_{r,j}$) and axial ($dF_{a,j}$) acting on the differential flute (j) element of height *dz* is acted as;

$$dF_{t,j}(\phi, z) = \left[K_{tc} h_j\left(\phi_j(z)\right) + K_{te}\right] dz \qquad 2.4\ (a)$$

$$dF_{r,j}(\phi, z) = \left[K_{rc} h_j\left(\phi_j(z)\right) + K_{re}\right] dz \qquad 2.4\ (b)$$

$$dF_{a,j}(\phi, z) = \left[K_{ac} h_j\left(\phi_j(z)\right) + K_{ae}\right] dz \qquad 2.4\ (c)$$

where K_{tc}, K_{rc}, K_{ac} are the cutting force coefficients in tangential, radial and axial direction respectively and K_{te}, K_{re}, K_{ae} are the edge constant which are taken in consideration because of rubbing and ploughing.

These elemental forces are resolved into feed (*x*), normal (*y*), and axial (z) directions using transformation as;

$$dF_{x,j}\left(\phi_j(z)\right) = dF_{t,j}\cos\phi_j(z) - dF_{r,j}\sin\phi_j(z) \qquad 2.5\ (a)$$

$$dF_{y,j}\left(\phi_j(z)\right) = dF_{t,j}\sin\phi_j(z) - dF_{r,j}\cos\phi_j(z) \qquad 2.5\ (b)$$

$$dF_{z,j}\left(\phi_j(z)\right) = dF_{a,j} \qquad 2.5\ (c)$$

The total cutting force produced by the flutes as:

$$F_q\left(\phi_j(z)\right) = \sum_{z_{j1}}^{z_{j2}} \Delta F_{qj}(\phi_j(z))\ \Delta z, \qquad q = x, y, z \qquad 2.6$$

where $z_{j1}(\phi_j(z))$ and $z_{j2}(\phi_j(z))$ are the lower and upper axial engagement limits of the in-cut portion of the flute j.

When more than one tooth cuts simultaneously, the contribution of each tooth to total feed, normal and axial forces must be considered. We can formulate the total feed, normal, and axial forces as:

$$F_x(\phi) = \sum_{j=0}^{N-1} F_{xj}\,; \qquad F_y(\phi) = \sum_{j=0}^{N-1} F_{yj}\,; \qquad F_z(\phi) = \sum_{j=0}^{N-1} F_{zj} \tag{2.7}$$

The resultant cutting force acting on the milling cutter is then calculated as;

$$\mathrm{F}(\phi) = \sqrt{\mathrm{F_x}(\phi)^2 + \mathrm{F_y}(\phi)^2 + \mathrm{F_z}(\phi)^2} \tag{2.8}$$

2.4 Chatter Modelling

External dynamic forces are common in actual cutting conditions, whether they are harmonic, periodic, or random. Dynamic milling introduces inherent force-induced vibrations at the tooth passing frequency, which under certain conditions, may influence the cutting process and cause self-induced or self-excited vibrations during machining. Chatter, or self-excited vibration, can occur during milling at specific axial depth of cut and spindle speed combinations. The wavy chip thickness is caused by relative displacement between the tool and workpiece, resulting from current and previous waviness. This type of instability is known as regenerative chatter. The phase difference between inner and outer waves can cause chips to accumulate exponentially, resulting in enormous forces and vibrations that cause the tool to jump out of the cut. This can lead to surface damage and/or tool failure, thus the researchers decided to model the chatter to determine stable machining parameters [6].

2.4.1 Dynamics of Milling

Milling tools contain two orthogonal degrees of freedom in the x and y directions, as seen in Fig. 2.5. The cutting forces excite the structure in both the feed (x) and normal (y) directions, resulting in dynamic displacements x and y. The chip thickness is made up of two parts: a static component from the cutter's rigid body motion and a dynamic component from the tool's vibrations during the tooth phase.

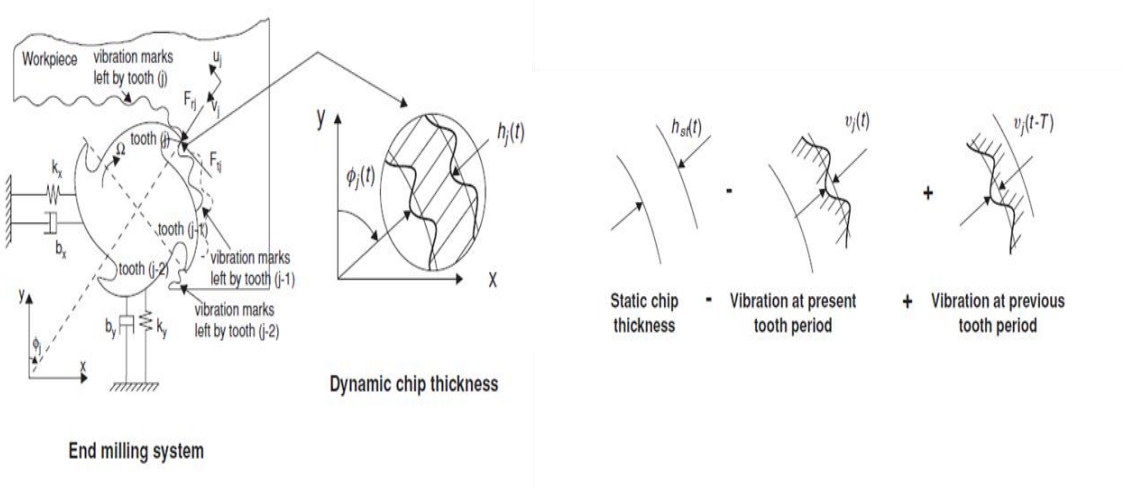

Fig. 2.5 Self excited vibrations in 2-DOF milling system [6]

Because the chip thickness is measured in the radial direction (v_j), the total chip load can be expressed by,

$$h(\phi_j) = \left[s_t sin\phi_j + \left(v_{j,0} - v_j\right)\right] g(\phi_j) \qquad 2.9$$

Where, s_t is the feed rate per tooth and $\left(v_{j,0} - v_j\right)$ are the dynamic displacements of the cutter at the previous and present tooth periods, respectively. The function is $g(\phi_j)$ a unit step function that determines whether the tooth is in or out of cut, that is,

$$g\left(\phi_j\right) = 1 \leftarrow \phi_{st} < \phi_j < \phi_{ex} ;$$

$$g\left(\phi_j\right) = 0 \leftarrow \phi_j < \phi_{st} \; or \; \phi_j > \phi_{ex}$$

Where, ϕ_{st} and ϕ_{ex} are the start and exit immersion angles. Only, the dynamic componentof the chip thickness will contribute to the dynamic chip load regeneration mechanism hence we neglect the static chip thickness. Hence the dynamic chip become as;

$$h(\phi_j) = [\Delta x \sin \phi_j + \Delta y \cos \phi_j] \, g(\phi_j) \qquad 2.10$$

where $\Delta x = x - x_0$ and $\Delta y = y - y_0$. Here, (x, y) and $(x_0 - y_0)$ represent the dynamic displacements of the cutter structure at the present and previous tooth periods, respectively.

The tangential (F_{tj}) and radial (F_{rj}) cutting forces acting on the tooth j can be expressed as;

$$F_{tj} = K_t a h(\phi_j)\,;\;\; F_{rj} = K_r F_{tj} \qquad 2.11$$

where cutting coefficients K_t and K_r are constant.

Resolving the cutting forces in the x and y directions,

$$F_{xj} = -F_{tj} cos\phi_j - F_{rj} sin\phi_j \qquad 2.12$$

$$F_{yj} = +F_{tj} sin\phi_j - F_{rj} cos\phi_j \qquad 2.13$$

Adding the cutting forces contributed by all the teeth, the total dynamic milling forces acting on the cutter is given by,

$$F_x = \sum_{j=0}^{N-1} F_{xj}(\phi_j); \qquad F_y = \sum_{j=0}^{N-1} F_{yj}(\phi_j); \qquad 2.14$$

Where, $\phi_j = \phi + j\phi_p$ and cutter pitch angle is $\phi_p = \frac{2\pi}{N}$.

Substituting chip thickness (2.10) and tooth forces (2.11), on rearranging expressions are expressed in form of a matrix;

$$\begin{bmatrix} F_x \\ F_y \end{bmatrix} = \frac{1}{2} a K_t \begin{bmatrix} a_{xx} & a_{xy} \\ a_{yx} & a_{yy} \end{bmatrix} \begin{bmatrix} \Delta x \\ \Delta y \end{bmatrix} \qquad 2.15$$

⬇

Time- varying directional matrix A[t]

The time dimensional dynamic milling coefficients are given as;

$$a_{xx} = \sum_{j=0}^{N-1} -g_j[sin2\phi_j + K_r(1 - cos2\phi_j)]$$

$$a_{xy} = \sum_{j=0}^{N-1} -g_j[(1 + cos2\phi_j) + K_r sin2\phi_j]$$

$$a_{yx} = \sum_{j=0}^{N-1} g_j[(1 - cos2\phi_j) - K_r sin2\phi_j]$$

$$a_{yy} = \sum_{j=0}^{N-1} g_j[sin2\phi_j - K_r(1 + cos2\phi_j)]$$

Considering that the angular position of the parameters changes with time and angular velocity Eq. 2.15 can be expressed in the time domain in a matrix form as,

$$\{F(t)\} = \frac{1}{2} a K_t [A(t)]\{\Delta(t)\} \quad 2.16$$

2.4.2 Frequency Domain Chatter Modelling

Altintas et al. [23] presented the frequency domain solution for the milling stability problem. The dynamic cutting force is converted from the time domain to the frequency domain by taking the Fourier transform of Eq. 2.16 as follows;

$$\{F(\omega)\} = \frac{1}{2} a K_t \{[A(\omega)] * \{\Delta(\omega)\}\} \quad 2.17$$

Where $*$ donates convolution integral & $\{\Delta(\omega)\}$ is difference of displacement between present and previous cut in frequency domain and defined as;

$$\{\Delta(\omega)\} = [1 - e^{-wT}][\Phi(w)]\{F(\omega)\} \quad 2.18$$

Where $[\Phi(w)]$ is the frequency response function matrix of the structure at the tool workpiece contact region. Hence dynamic milling force equation in frequency domain as;

$$\{F(\omega)\} = \frac{1}{2} a K_t \{[A(\omega)] * [1 - e^{-\omega T}][\Phi(\omega)]\{F(\omega)\} \quad 2.19$$

For zero-order solution the force equation become;

$$\{F(\omega)\} = \frac{1}{2} a K_t \{[A_0][1 - e^{-\omega T}][\Phi(\omega)]\{F(\omega)\} \quad 2.20$$

$$\frac{N}{2\pi}\begin{bmatrix}\alpha_{xx} & \alpha_{xy}\\ \alpha_{yx} & \alpha_{yy}\end{bmatrix}$$

$$a_{xx} = \frac{1}{2}[cos2\phi - 2K_r + K_r sin2\phi]_{\phi_{st}}^{\phi_{ex}}$$

$$a_{xy} = \frac{1}{2}[-sin2\phi - 2\phi + K_r cos2\phi]_{\phi_{st}}^{\phi_{ex}}$$

$$a_{yx} = \frac{1}{2}[-sin2\phi + 2\phi + K_r cos2\phi]_{\phi_{st}}^{\phi_{ex}}$$

$$a_{yy} = \frac{1}{2}[-cos2\phi - 2K_r\phi - K_r sin2\phi]_{\phi_{st}}^{\phi_{ex}}$$

If the system is critically stable at the chatter frequency ω_c , the stability of system is defined by the following characteristic equation,

$$det|[I] - \Lambda_1[\Phi_0(i\omega_c)]| = 0 \qquad 2.21$$

Where, $[\Phi_0(i\omega_c)] = [A_0][\Phi(i\omega_c)]$ and $\Lambda = \Lambda_R + \Lambda_I = -\frac{N}{4\pi} aK_t\left(1 - e^{-i\omega_c T}\right)$

By solving characteristic equation 2.21, the final expression for chatter free axial depth of cut (a_{lim}) and spindle speed (n) is given as;

$$a_{lim} = -\frac{2\pi\Lambda_R}{NK_t}\left(1 + \left(\frac{\Lambda_I}{\Lambda_R}\right)^2\right) \qquad 2.22$$

Where K_t is cutting force coefficient.

$$n = \frac{60}{NT}; \quad T = \frac{1}{w_c}(\epsilon + 2k\pi) \qquad 2.23$$

Where ϵ is the phase shift between the inner and outer modulations and k is integer number of full vibration waves (lobes) in one tooth passing period (T).

2.5 Research Gap

Significantly, chatter vibrations in ball end micro milling have been relatively understudied, primarily due to the complex geometry and dynamic chip load generation mechanism. Hence, following gap are in the field of ball end micro milling as:

- Dynamic Modelling: Need for dynamic model to predict and control chatter in ball end micro milling, considering the unique dynamics of micro-scale operations.
- Parameter Optimization: Insufficient research on parameter optimization for milling complex 3D geometries and freeform surfaces using ball end micro mills.
- Surface Finish: Existing studies often lack comprehensive characterization of surface roughness in ball end micro milling, particularly for complex 3D surfaces and intricate geometries.
- Material Behavior: Understanding how microstructural features, such as grain size and phase distribution, affect the milling process is essential for accurate modeling and

optimization.

- Tool Wear: Limited research on tool wear behavior in ball end micro milling, particularly concerning the interaction between cutting parameters and tool wear characteristics.

2.6 Objective of the Present Study

The following are specific objectives that may be examined within the framework of such a thesis:

- Force Model Development: Develop the computational models to calculate the cutting forces in ball end micro milling processes.
- Chatter Model Development: Develop a chatter prediction model that can determine the likelihood of chatter or non-chatter zone during ball end micro milling.
- Parameter Optimization: Investigate how different cutting parameters can affect cutting forces and stability in ball end micro milling. Optimize these parameters to maximize machining efficiency while avoiding chatter.

The overall goal of the thesis is to enhance the understanding of ball end micro milling processes. And find the cutting forces generated during ball end micro milling machining processes. Also find the chatter and non-chatter zone to improved machining practices, and potentially reduce costs and improve product quality in manufacturing industries.

CHAPTER 3

METHODOLOGY

This chapter provides a detailed overview of the steps and methodologies employed to achieve the research objectives. The goal of the research is to determine chatter in ball end micro milling. The modelling methodology is used to creates a predictive model for chatter in ball end micro milling by combining theoretical and analytical approaches. To achieve this intricate relationship between the milling tool, workpiece and machining parameters that causes chatter are thoroughly explored.

3.1 Geometric Modelling of Ball End Milling

Every cutting edge on the tool has been carefully designed to offer optimal cutting performance while reducing the generated cutting forces. A detailed analysis of the cutting-edge geometry is also necessary for the development of the force model. In ball end mills, the exact description of the cut geometry is complicated because the points along the cutting edge generate trochoid curves. The ball-end mill cutter is composed of the ball part and the end mill part. The detailed geometry for ball end mill is shown in Fig. 3.1. Since this cutting edge is sitting on the spherical surface, the cutting condition is different at every point along the edge. Each flute lies on the surface of the hemisphere, and is ground with a constant helix lead. The flutes have a helix angle of β at the ball-shank meeting boundary. Due to the reduction of radius at (x-y) planes towards the ball tip in axial (z) direction, the local helix angle $\beta(\psi)$ along the cutting flute varies for constant helix-lead cutters. The ball part of the cutter meets with a cylindrical shank which has a radius of R_0 and the ball radius is the same.

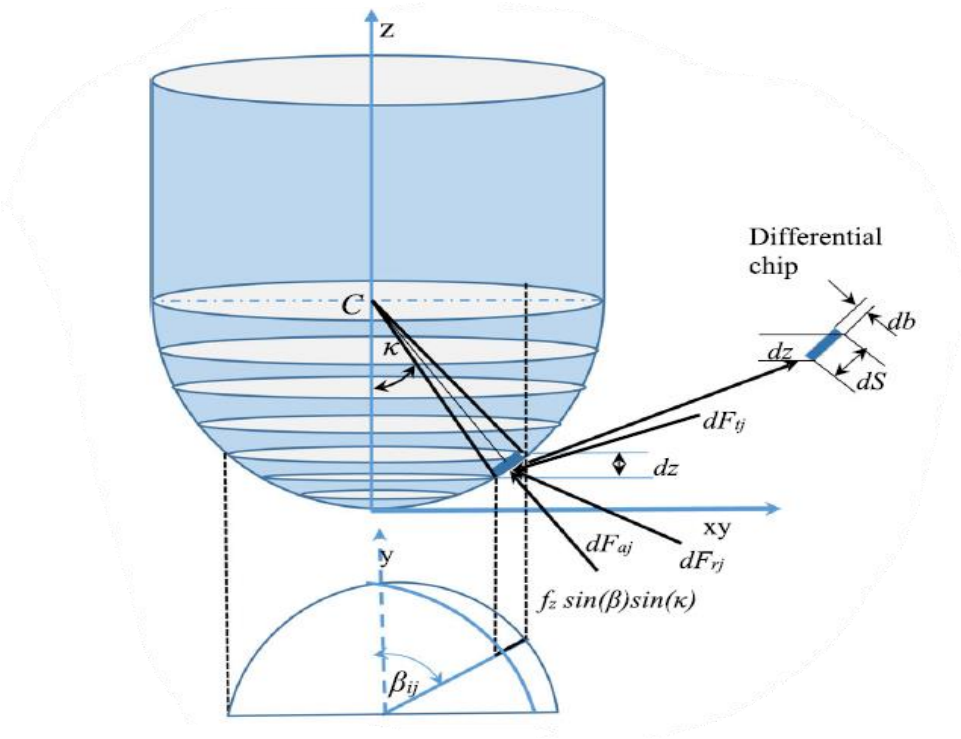

Fig. 3.1 Geometry of ball end mill

The expression for the envelope of the ball part is given by,

$$x^2 + y^2 + (z - R_0)^2 = R_o^2 \qquad 3.1$$

where R_0 is the ball radius of the cutter measured from the centre of the sphere (C).

The cutter radius in x-y plane at axial location z is,

$$R^2(z) = x^2 + y^2 \qquad 3.2$$

and it is zero at the ball tip. The z coordinate of a point located on the cutting edge is,

$$z = \frac{R_0 \psi}{\tan \beta} \qquad 3.3$$

Where ψ is the lag angle between the tip of the flute at z = 0 and at axial location z.

From the equations given above, the cutter radius in x - y plane, which touches a point on the helical and spherical flute located at angle ψ, can be expressed as,

$$R(\psi) = R_0\sqrt{1 - (\psi \cot\beta - 1)^2} \quad 3.4$$

3.2 Cutting Force Modelling of Ball End Milling

Ball end milling, a subset of end milling, uses a hemispherical end mill to create three-dimensional contours and profiles. The forces generated during this process are complex due to the varying cutting-edge engagement along the tool's spherical surface. Understanding these forces is crucial for predicting tool deflection, vibration (including chatter), and surface finish. Cutting force modelling essential for predicting the performance and optimizing the milling process. Development of a cutting force model for ball end milling is presented in next section.

3.2.1 Mechanistic Force Modelling

Ball end milling tool consist ball part and end mill part in its geometry. Points along the cutting edge in ball end milling generate trochoid curves. Along the cutting edge, there are variations in the cutting condition everywhere. The cutting edge is situated on a spherical portion. With a change in the axial location of the cutting-edge section in contact with the workpiece, the cutting edge's effective radius also varies. This results from the spherical part's changing helix angle. The cutting force for a given workpiece/cutter combination may be easily determined by utilising the empirical chip-force correlations once the chip geometry for that particular cutter orientation has been established through the cutting engagement test and chip thickness determination technique. Fig. 3.2 depicts the ball end milling operation, including cutting forces and chip thickness variations.

In ball end milling the instantaneous chip thickness (h) varies periodically as a function of radial immersion angle (β) and axial immersion angle (k). The chip thickness variation can be approximated as:

$$h(\beta, \psi, k) = f_z \sin\beta \sin k \quad 3.5$$

where f_z is the feed rate (mm/rev-tooth)

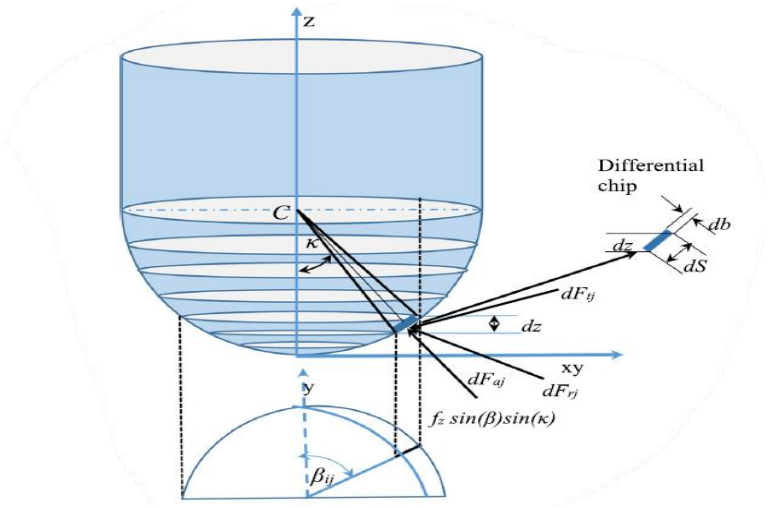

Fig. 3.2 Chip thickness variation and cutting forces in ball end milling

The cutting edge of a ball end mill is evenly discretized into a finite number of discs along the cutter's axis in order to evaluate cutting forces. The discretization of the cutting edge makes it possible to simplify the cutting edge as a series of linear cutting segments. The cutting edge can be characterized by the axial position (z) from the tool tip, radial distance (R_z) from the cutter axis, axial immersion angle (κ), and radial immersion angle (β) as shown in Fig. 3.3.

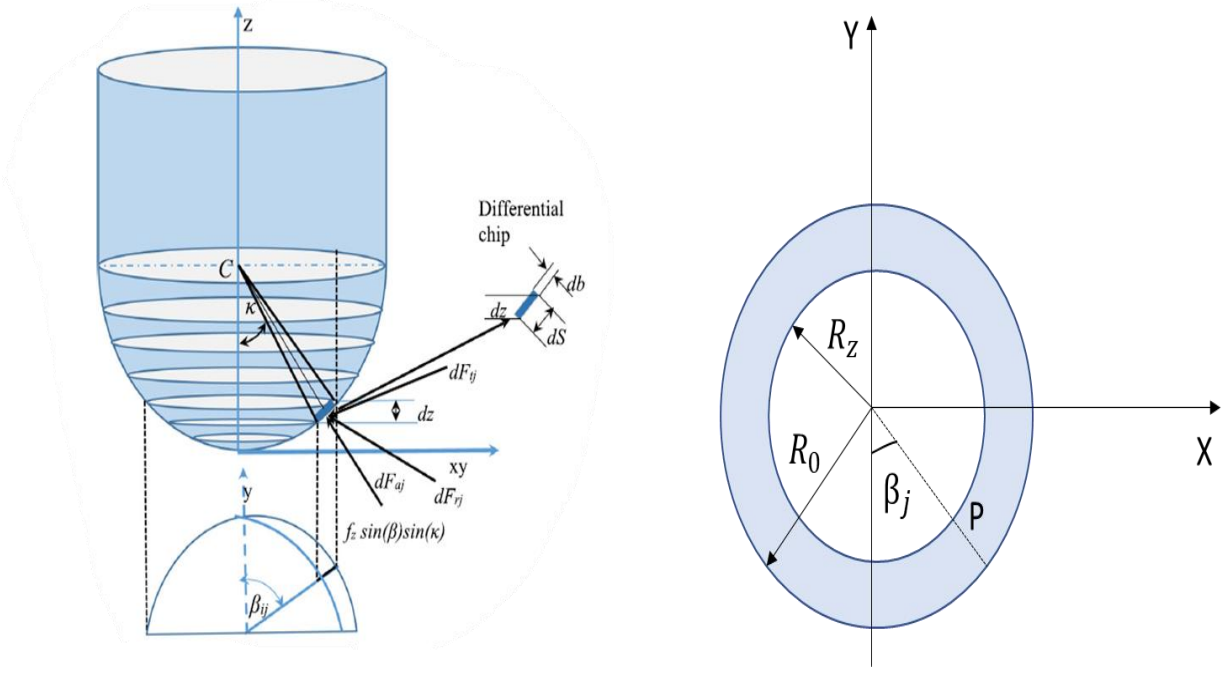

Fig. 3.3 Front view of the discretized cutter and top view with position angles

Position of the i^{th} element on the j^{th} cutting edge with elevation as the function of radial position angle (β), lag angle (ψ), and effective radius (R_z) may be given as follows:

$$x_{ij} = R_z \sin \beta_{ij} \quad 3.6$$

$$y_{ij} = R_z \cos \beta_{ij} \quad 3.7$$

$$z_{ij} = \frac{R_0 \psi}{\tan i_0} \quad 3.8$$

where R_0 is the ball radius of the cutter measured from the center of the sphere (C) and i_0 is helix angle.

If bottom end of one tooth is at an immersion angle β then the other tooth's immersion angle at the same instant will be;

$$\beta_j(0) = \beta + j\phi_p \quad ; \quad j = 0,1,2, \ldots\ldots\ldots(N-1) \quad 3.9$$

Where,

$$\phi_p(\text{tooth spacing angle}) = \frac{2\pi}{N}$$

The immersion angle for flute j (where j = 0,1, 2, …(N-1)) at an axial depth of cut z will depend on lag angle $\psi = k_\beta z$, where $k_\beta = \frac{\tan i_0}{R_0}$ and is given by,

$$\beta_j(z) = \beta + j\phi_p - k_\beta z \quad 3.10$$

The elemental tangential $(dF_{t,j})$, radial $(dF_{r,j})$, and axial $(dF_{a,j})$ cutting forces acting on the cutter are given by,

$$dF_t(\beta, z) = [K_{tc} h(\beta, \psi, k) db + K_{te} ds] \quad 3.11 \text{ (a)}$$

$$dF_r(\beta, z) = [K_{rc} h(\beta, \psi, k) db + K_{re} ds] \quad 3.11 \text{ (b)}$$

$$dF_a(\beta, z) = [K_{ac} h(\beta, \psi, k) db + K_{ae} ds] \quad 3.11 \text{ (c)}$$

where K_{tc}, K_{rc}, K_{ac} are the cutting force coefficients in tangential, radial and axial direction respectively and K_{te}, K_{re}, K_{ae} are the edge constant which are taken in consideration because of rubbing and ploughing.

Where, db is the differential cutting width is the projected length of infinitesimal cutting flute in the direction of cutting velocity and given as,

$$db = \frac{dz}{\sin k}$$

ds is the differential cutting edge length given as which can be given by the position vector of elemental cutting edge *P*.

$$ds = \sqrt{(R^{'}(\psi))^2 + R^2(\psi) + R_0^2 \cot {i_0}^2}\, d\psi$$

Where,

$$R(\psi) = R_0\sqrt{1 - (\psi \cot i_0 - 1)^2}$$

$\left(R^{'}(\psi)\right)$ is the derivate of $R(\psi)$ w.r.t ψ.

These elemental forces are resolved into feed (*x*), normal (*y*), and axial (z) directions using transformation matrix $[T]$ as;

$$\{dF_{xyz}\} = [T]\{dF_{rta}\}$$

$$\begin{bmatrix} dF_x \\ dF_y \\ dF_z \end{bmatrix} = \begin{bmatrix} -\sin(k)\sin(\psi) & -\cos(\psi) & -\cos(k)\sin(\psi) \\ -\sin k\cos(\psi) & \sin\psi & -\cos(k)\cos(\psi) \\ \cos(k) & 0 & -\sin(k) \end{bmatrix} \begin{bmatrix} dF_r \\ dF_t \\ dF_a \end{bmatrix} \qquad 3.12$$

The total cutting forces acting on one flute with an axial depth of cut z is given as;

$$F_q\left(\beta_j(z)\right) = \sum_{z_{j1}}^{z_{j2}} \Delta F_{qj}(\beta_j(z))\ \Delta z, \qquad \text{q = x, y, z} \qquad 3.13$$

where $z_{j1}(\beta_j(z))$ and $z_{j2}(\beta_j(z))$ are the lower and upper axial engagement limits of the in-cut portion of the flute j.

If more than one tooth cuts simultaneously, the contribution of each tooth to total feed, normal and axial forces must be considered. We can formulate the total feed, normal, and axial forces as:

$$F_x(\beta) = \sum_{j=0}^{N-1} F_{xj}\,; \qquad F_y(\beta) = \sum_{j=0}^{N-1} F_{yj}\,; \qquad F_z(\beta) = \sum_{j=0}^{N-1} F_{zj} \qquad 3.14$$

The resultant cutting force acting on the milling cutter is then calculated as;

$$\mathrm{F}\,(\beta) = \sqrt{\mathrm{F_x}(\beta)^2 + \mathrm{F_y}(\beta)^2 + \mathrm{F_z}(\beta)^2} \qquad 3.15$$

In order to calculate the cutting forces, the flow chart is given in Fig. 3.4 for ball end mill.

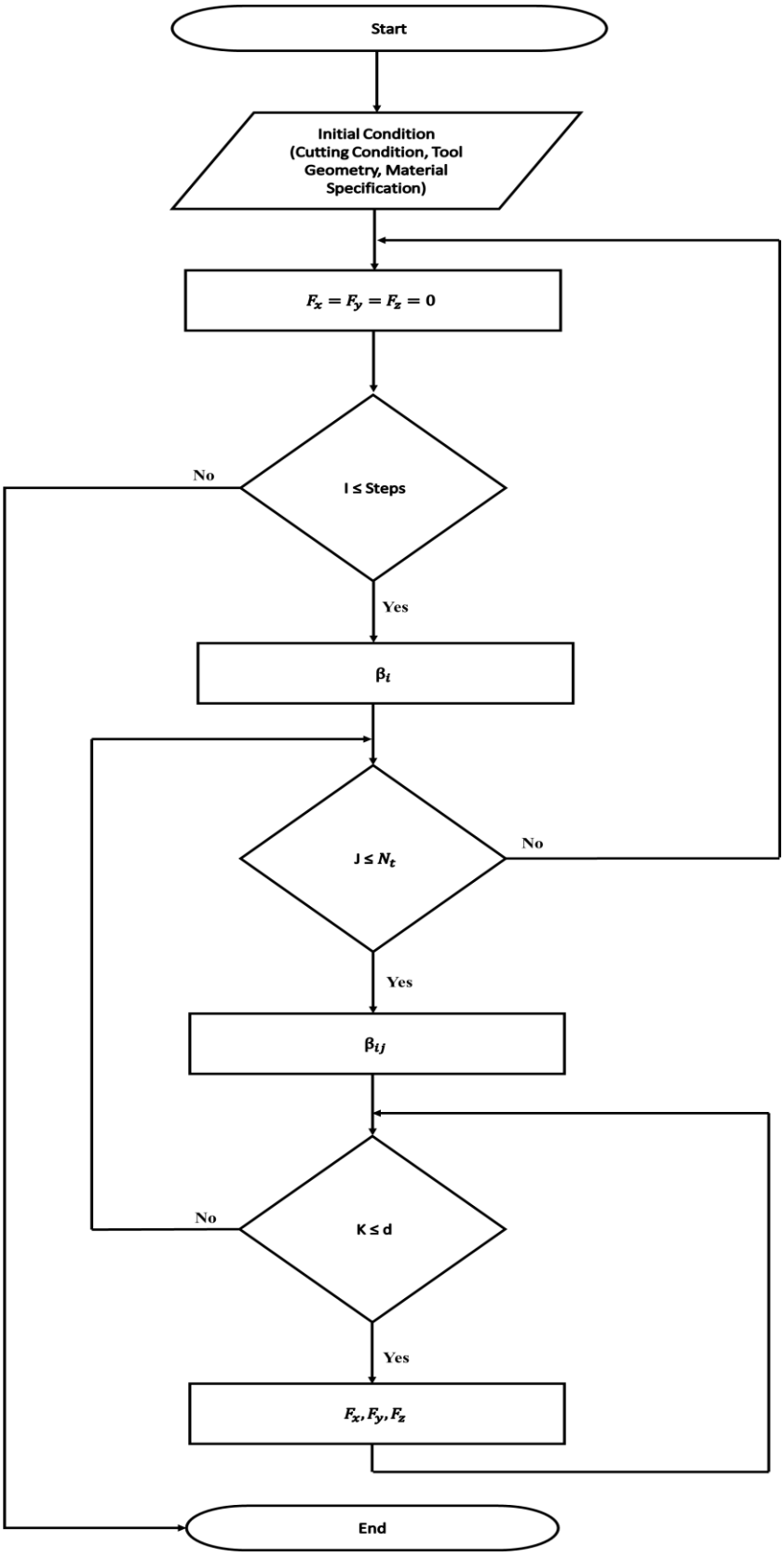

Fig. 3.4 Flow chart for cutting force calculation

3.3 Chatter Modelling of Ball End Milling

Chatter, a self-excited vibration phenomenon, significantly affects the surface finish, tool life, and machining accuracy in ball end micro milling. Chatter occurs due to the dynamic interaction between the cutting tool and the workpiece, leading to unstable cutting conditions. Chatter is often caused by the regenerative effect, where vibrations from previous cutting passes affect the current pass. Due the flexibility of the tool, it vibrates which leaves the waviness in the cutting surface. In every rotation of tool, it generates new surface and every surface is wavy surface. If there is some phase difference between the previous and present cut then the chip thickness variation will occur which causes the regenerative chatter. Displacement between the tool and the workpiece modulates the chip thickness, influencing the cutting forces. Further this force excites the machine-tool system and make it unstable also affects the surface finish, tool life, and machining accuracy. Hence analysis of chatter become essential to get the stability in the system. Fig. 3.5 presents the schematic for stability analysis. In ball end micro milling, chatter modelling involves understanding the tool-workpiece dynamics, stability analysis, and the influence of machining parameters.

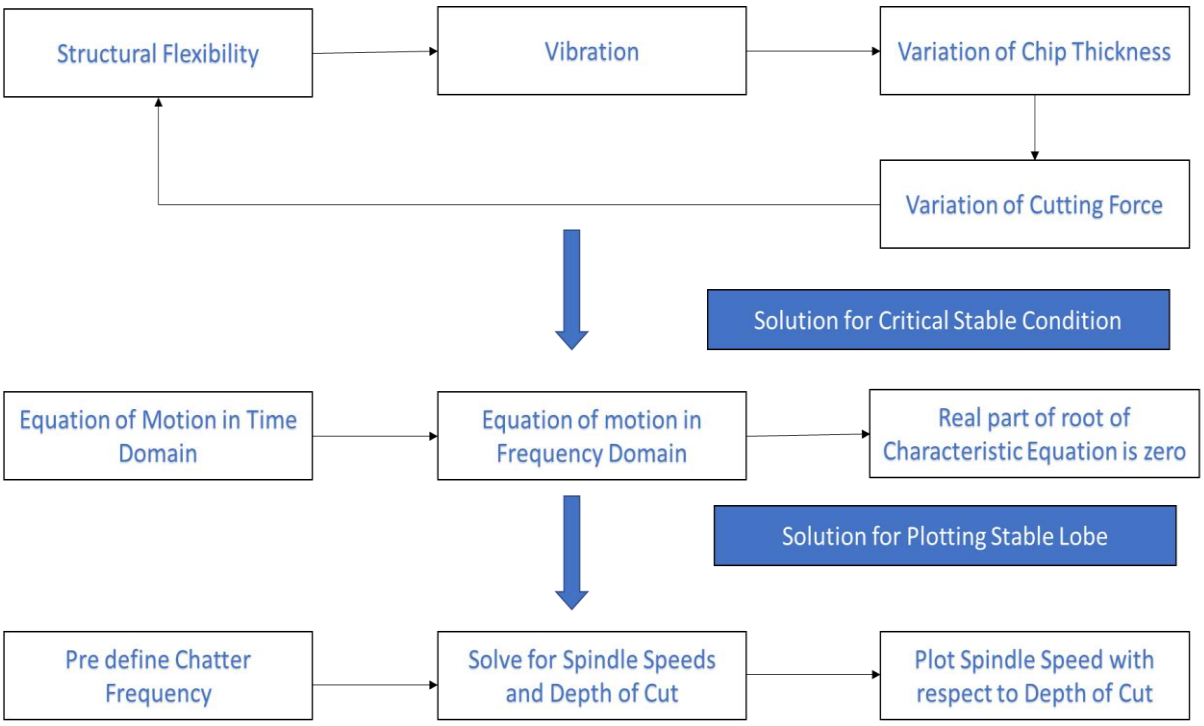

Fig. 3.5 Schematic for stability analysis

3.3.1 Dynamics of Milling

The ball end milling tools contain two degrees of freedom in the x and y directions, as seen in Fig. 3.6. The cutting forces excite the structure in both the feed (x) and normal (y) directions, resulting in dynamic displacements x and y. The chip thickness is made up of two parts: a static component from the cutter's rigid body motion and a dynamic component from the tool's vibrations during the tooth phase.

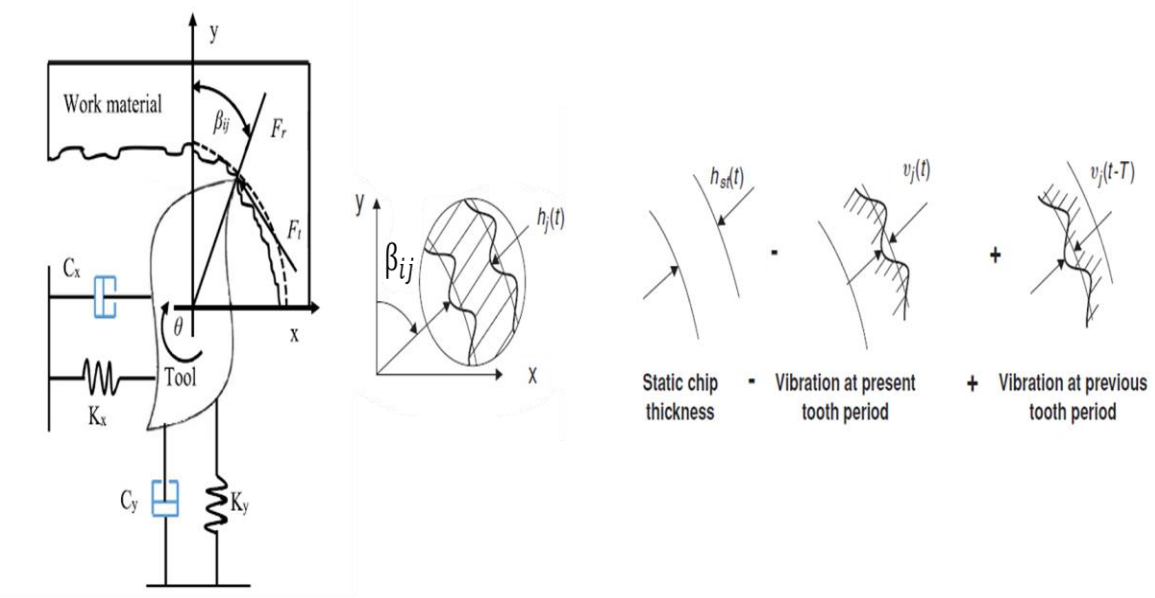

Fig. 3.6 Self excited vibrations in 2-DOF in ball end milling system

Because the chip thickness is measured in the radial direction (v_j), the total chip load can be expressed by

$$h(\beta_j) = \left[s_t sin\beta_j \sin k + \left(v_{j,0} - v_j\right)\right] g(\beta_j) \qquad 3.16$$

Where, s_t is the feed rate per tooth and $\left(v_{j,0} - v_j\right)$ are the dynamic displacements of the cutter at the previous and present tooth periods, respectively. The function is $g(\beta_j)$ a unit step function that determines whether the tooth is in or out of cut, that is

$$g(\beta_j) = 1 \leftarrow \beta_{st} < \beta_j < \beta_{ex} ;$$

$$g(\beta_j) = 0 \leftarrow \beta_j < \beta_{st} \; or \; \beta_j > \beta_{ex}$$

Where, β_{st} and β_{ex} are the start and exit immersion angles. Only, the dynamic componentof the chip thickness will contribute to the dynamic chip load regeneration mechanism hence we neglect the static chip thickness. Hence the dynamic chip become as

$$h(\beta_j) = [\Delta x \sin\beta_j \sin k + \Delta y \cos\beta_j \sin k]\, g(\beta_j) \qquad 3.17$$

where $\Delta x = x - x_0$ and $\Delta y = y - y_0$. Here, (x, y) and $(x_0 - y_0)$ represent the dynamic displacements of the cutter structure at the present and previous tooth periods, respectively.

The tangential (F_{tj}) and radial (F_{rj}) cutting forces acting on the tooth j can be expressed as

$$dF_t = K_{tc} h(\beta, \psi, k) db \qquad 3.18\ (a)$$

$$dF_r = K_{rc} h(\beta, \psi, k) db \qquad 3.18\ (b)$$

where cutting coefficients K_{tc} and K_{rc} are constant.

Resolving the cutting forces in the x and y directions

$$\begin{bmatrix} F_x \\ F_y \end{bmatrix} = \begin{bmatrix} -\sin\beta \sin k & -\cos\beta \\ -\cos\beta \sin k & \sin\beta \end{bmatrix} \begin{bmatrix} dF_r \\ dF_t \end{bmatrix} \qquad 3.19$$

Adding the cutting forces contributed by all the teeth, the total dynamic milling forces acting on the cutter is given by

$$F_x = \sum_{j=0}^{N-1} F_{xj}(\beta_j); \qquad F_y = \sum_{j=0}^{N-1} F_{yj}(\beta_j); \qquad 3.20$$

Substituting chip thickness (3.17) and tooth forces (3.18 (a, b)), on rearranging expressions are expressed in form of a matrix

$$\begin{bmatrix} F_x \\ F_y \end{bmatrix} = \frac{1}{2} a_p \begin{bmatrix} a_{xx} & a_{xy} \\ a_{yx} & a_{yy} \end{bmatrix} \begin{bmatrix} \Delta x \\ \Delta y \end{bmatrix} \qquad 3.21$$

⬇

Time- varying directional matrix A[t]

The time dimensional dynamic milling coefficients are given as

$$a_{xx} = \sum_{j=0}^{N-1} -g_j[K_{ts} sin2\beta_j + K_{rs}\, sin\, k\,(1 - cos2\beta_j)]$$

$$a_{xy} = \sum_{j=0}^{N-1} -g_j[K_{ts}(1 + cos2\beta_j) + K_{rs}\, sin\, k\, sin2\beta_j]$$

$$a_{yx} = \sum_{j=0}^{N-1} g_j[K_{ts}(1 - cos2\beta_j) - K_{rs}\, sin\, k\, sin2\beta_j]$$

$$a_{yy} = \sum_{j=0}^{N-1} g_j[K_{ts} sin2\beta_j - K_{rs}\, sin\, k\,(1 + cos2\beta_j)]$$

Considering that the angular position of the parameters changes with time and angular velocity Eq. 3.21 can be expressed in the time domain in a matrix form as

$$\{F(t)\} = \frac{1}{2} a K_t [A(t)]\{\Delta(t)\} \qquad 3.22$$

3.3.2 Frequency Domain Chatter Modelling

The dynamic cutting force is converted from the time domain to the frequency domain by taking the Fourier transform of Eq. 3.22 as follows

$$\{F(\omega)\} = \frac{1}{2} a_p \{[A(\omega)] * \{\Delta(\omega)\}\} \qquad 3.23$$

Where $*$ donates convolution integral & $\{\Delta(\omega)\}$ is difference of displacement between present and previous cut in frequency domain and defined as

$$\{\Delta(\omega)\} = [1 - e^{-wT}][\Phi(w)]\{F(\omega)\} \qquad 3.24$$

Where $[\Phi(w)]$ is the frequency response function matrix of the structure at the tool workpiece contact region. Hence dynamic milling force equation in frequency domain as

$$\{F(\omega)\} = \frac{1}{2} a_p \{[A(\omega)] * [1 - e^{-\omega T}][\Phi(\omega)]\{F(\omega)\} \qquad 3.25$$

To solve this using zero-order approximation solution of the force equation become

$$\{F(\omega)\} = \frac{1}{2} a_p \{[A_0][1 - e^{-\omega T}][\Phi(\omega)]\{F(\omega)\} \quad 3.26$$

$$\downarrow$$

$$\frac{N}{2\pi}\begin{bmatrix}\alpha_{xx} & \alpha_{xy}\\ \alpha_{yx} & \alpha_{yy}\end{bmatrix}$$

$$a_{xx} = \frac{1}{2}[K_{ts}cos2\beta - K_{rs}\, sin\, k\,(2\beta - sin2\beta)]_{\beta_{st}}^{\beta_{ex}}$$

$$a_{xy} = \frac{1}{2}[-2K_{ts}\beta - K_{ts}sin2\beta + K_{rs}\, sin\, k\, cos2\beta]_{\beta_{st}}^{\beta_{ex}}$$

$$a_{yx} = \frac{1}{2}[2K_{ts}\beta - K_{ts}sin2\beta + K_{rs}\, sin\, k\, cos2\beta]_{\beta_{st}}^{\beta_{ex}}$$

$$a_{yy} = \frac{1}{2}[-K_{ts}cos2\beta - K_{rs}\, sin\, k\,(2\beta + sin2\beta)]_{\beta_{st}}^{\beta_{ex}}$$

If the system is critically stable at the chatter frequency ω_c , the stability of system is defined by the following characteristic equation

$$det\big[[I] - \Lambda_1[\Phi_0(i\omega_c)]\big] = 0 \quad 3.27$$

Where $[\Phi_0(i\omega_c)] = [A_0][\Phi(\omega_c)]$ and $\Lambda = \Lambda_R + \Lambda_I = -\frac{N}{4\pi} a_p\big(1 - e^{-i\omega_c T}\big)$

By solving characteristic equation 3.27, the final expression for chatter free axial depth of cut (a_{lim}) and spindle speed (n) is given as

$$a_{lim} = -\frac{\pi\Lambda_R}{N}\left(1 + \left(\frac{\Lambda_I}{\Lambda_R}\right)^2\right) \quad 3.28$$

$$n = \frac{60}{NT}; \qquad T = \frac{1}{w_c}(\epsilon + 2k\pi)$$

$$\varepsilon = \pi - 2\tan^{-1}\left(\frac{\Lambda_I}{\Lambda_R}\right)$$

$$n = \frac{60 w_c}{N(2k\pi + \epsilon)} \quad 3.29$$

where ϵ is the phase shift between the inner and outer modulations and k is integer number of full vibration waves (lobes) in one tooth passing period(T).

In order to find chatter and non-chatter using stability lobe diagram, the flow chart is given in Fig. 3.7. for ball end mill.

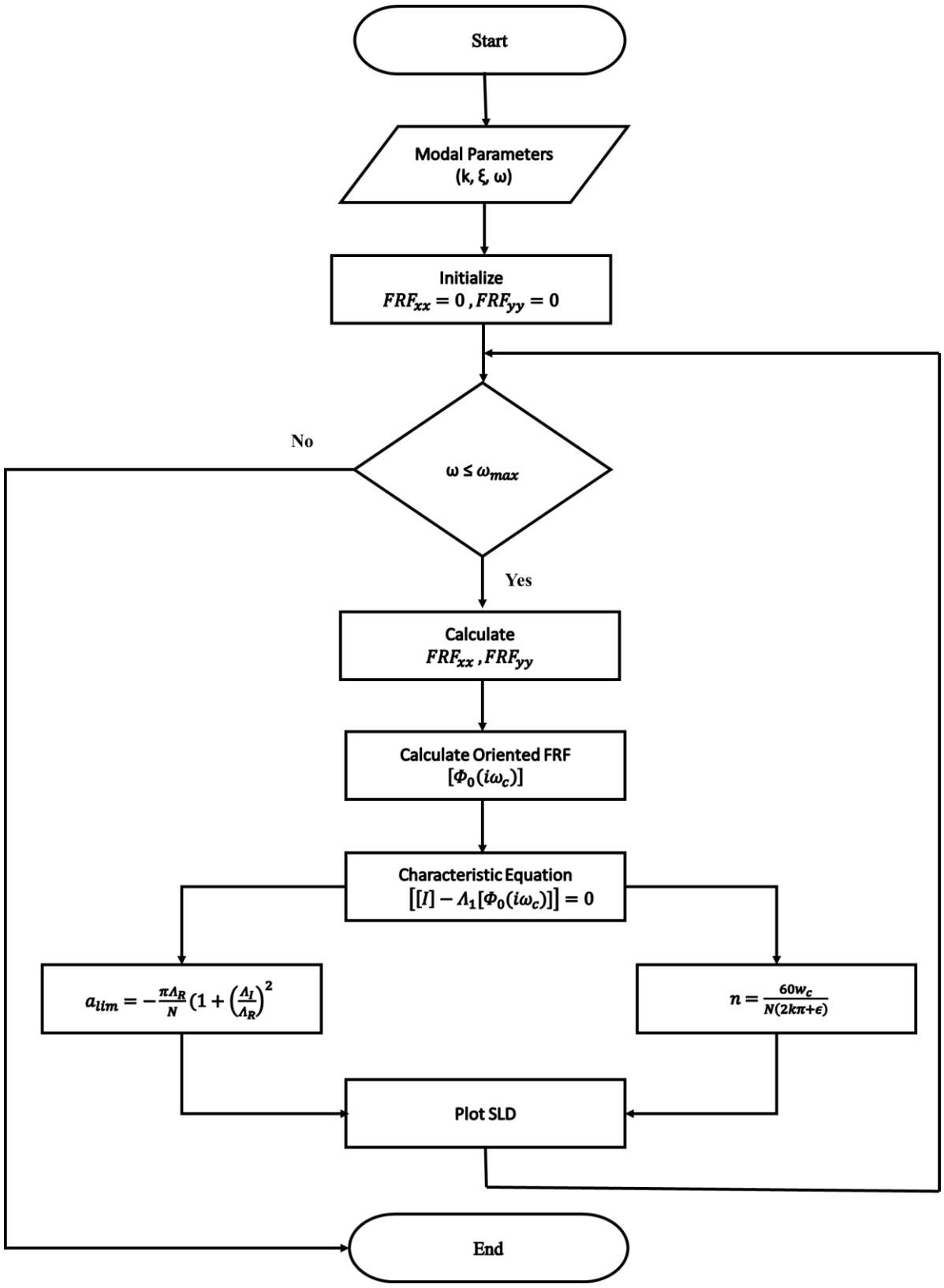

Fig. 3.7 Flow chart for stability lobe diagram

CHAPTER 4

RESULTS AND DISCUSSION

This chapter gives the chatter modelling results for ball end micro milling. Using MATLAB, cutting force model and chatter model is created. First, we created a force model to calculate forces in milling using a ball end mill. By executing the code, we can visualize how forces in x, y and z direction change dynamically throughout the milling process. For stability analysis chatter model is developed. By executing the chatter model, we identified the chatter and non-chatter zone at different spindle speed and depth of cut. Fig. 4.1 shows the forces at a given cutting condition [10]. Fig. 4.2 show the force model results. From observation we find the good agreement between them.

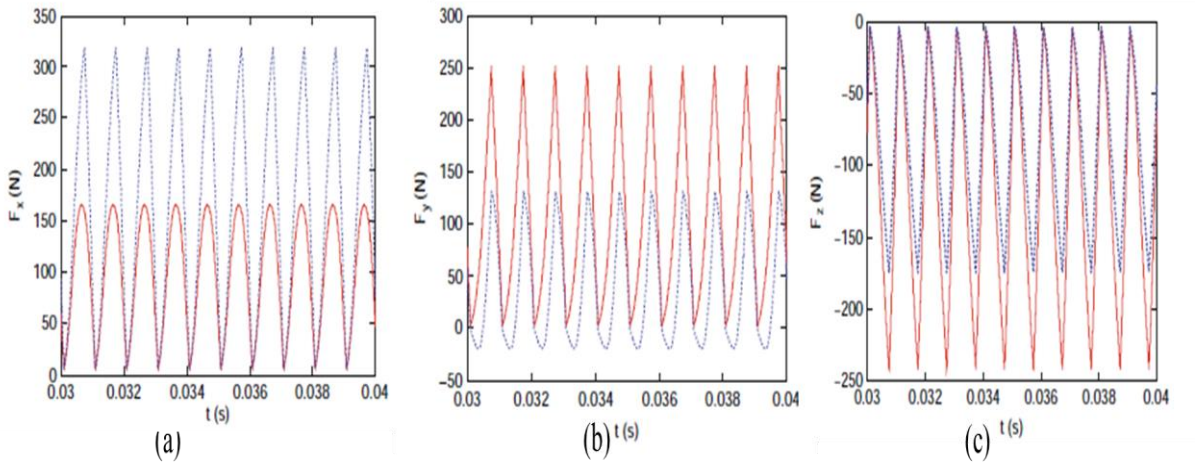

Fig. 4.1 Cutting Forces variation [10], (a) x-direction (b) y-direction (c) z-direction

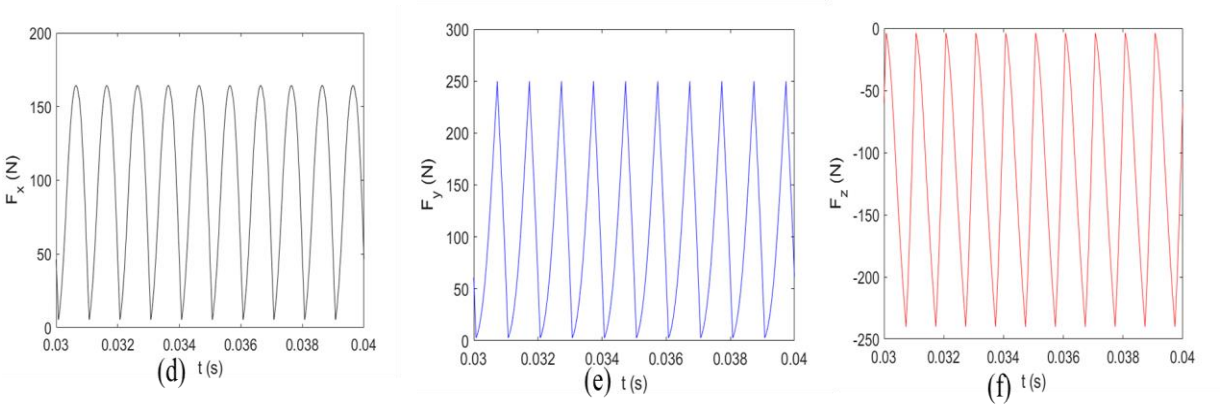

Fig. 4.2 Force model cutting forces variation (d) x-direction (e) y-direction (f) z-direction

4.1 Effect of Feed Rate on Cutting Forces

Feed rate is a crucial parameter in ball end milling that significantly influences the cutting forces and overall machining performance. This section examines the impact of varying feed rates on the cutting forces, drawing comparisons between them. Table 4.1 show the test cutting condition for cutting force analysis.

Test 1	**Test 2**	**Test 3**
D = 300 µm	D = 300 µm	D = 300 µm
$s_t = \frac{1\mu m}{\text{tooth} - \text{rev}}$	$s_t = \frac{2\mu m}{\text{tooth} - \text{rev}}$	$s_t = \frac{3\mu m}{\text{tooth} - \text{rev}}$
N = 2	N = 2	N = 2
z = 10 µm	z = 10 µm	z = 10 µm
n =15000 rpm	n =15000 rpm	n =15000 rpm

Table 4.1 Feed rate test cutting condition for force analysis

For the test 1, cutting force variation during machining is shown in fig. 4.3. From the figure it can be observed that load is periodical in x, y, z direction. The maximum value of force in x direction is 0.2 N and minimum is -0.77 N. In y- direction the maximum value of load is 0.84 N and minimum is -0.08 N and in z- direction the maximum value off load is 0 N and minimum is -0.9 N.

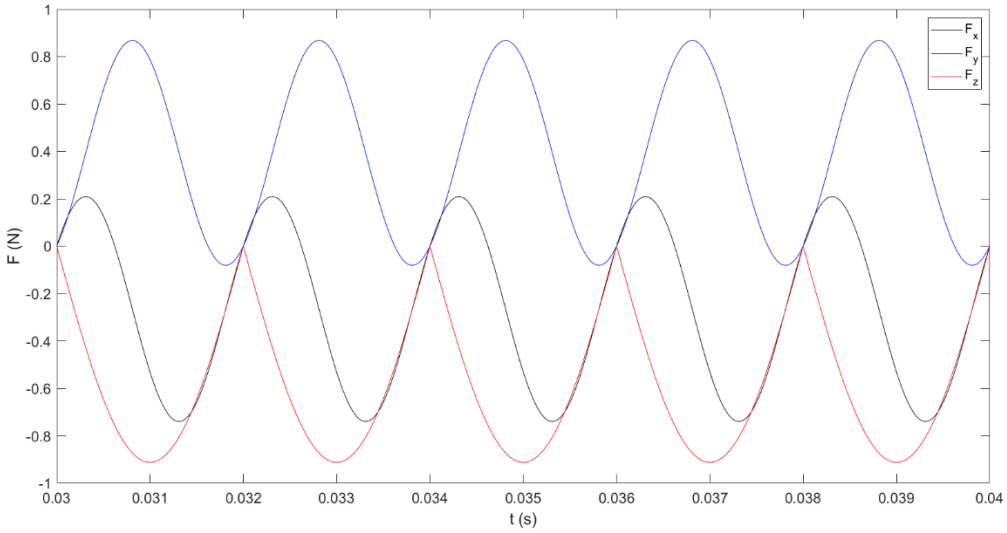

Fig. 4.3 Cutting forces variation for test 1

For the test 2, cutting force variation during machining is shown in fig. 4.4. From the figure it can be observed that load is periodical in x, y, z direction. The maximum value of force in x direction is 0.47 N and minimum is -1.5 N. In y- direction the maximum value of load is 1.7 N and minimum is -0.2 N and in z- direction the maximum value off load is 0 N and minimum is -1.8 N.

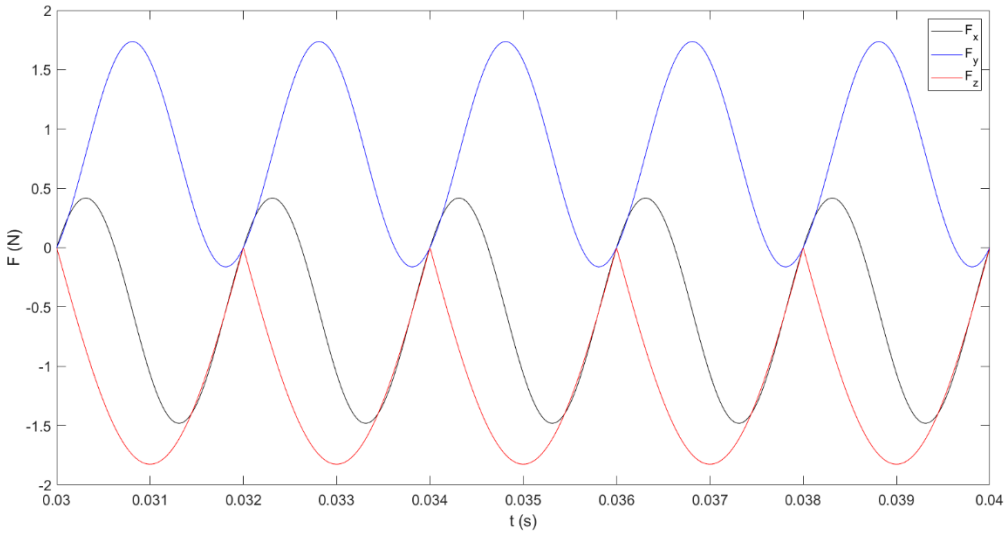

Fig. 4.4 Cutting forces variation for test 2

For the test 3, cutting force variation during machining is shown in fig. 4.5. From the figure it can be observed that load is periodical in x, y, z direction. The maximum value of force in x direction is 0.52 N and minimum is -2.18 N. In y- direction the maximum value of load is 2.6 N and minimum is -0.36 N and in z- direction the maximum value off load is 0 N and minimum is -2.7 N.

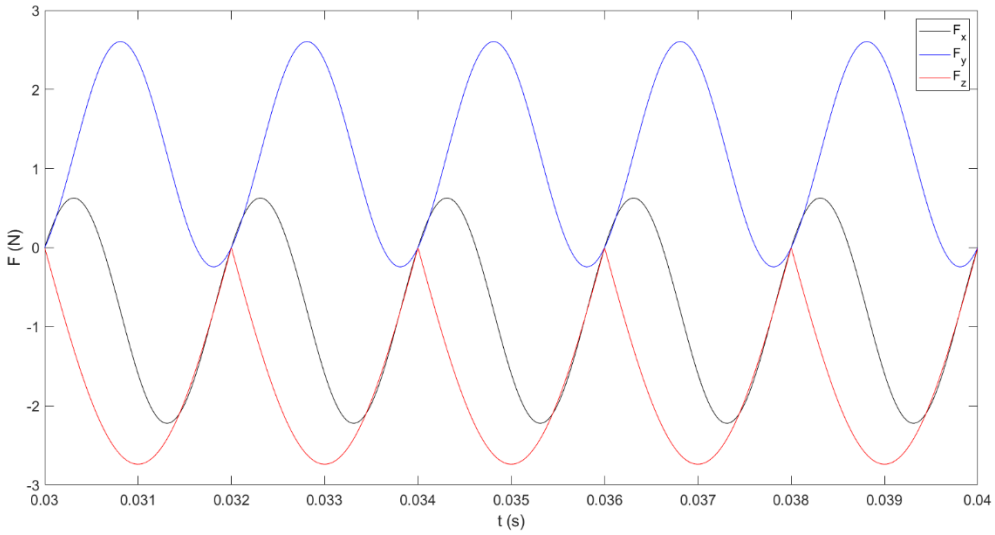

Fig. 4.5 Cutting forces variation for test 3

Testing of the forces variation over a wide range of feed rate conditions is analysed in ball end micro milling. Test are for the slot cutting condition. The investigation into the effect of feed rate on cutting forces confirms that higher feed rates result in increased cutting forces. The increase in cutting forces with higher feed rates can be attributed to the larger volume of material removed per unit time. As the feed rate increases, the chip load on each cutting-edge increase, leading to higher cutting forces. These force modelling results provide a comprehensive understanding of the dynamic forces acting on the ball end mill during the machining process. The variations observed underscore the importance of carefully selecting and optimizing cutting parameters to achieve desired machining outcomes while maintaining process stability.

4.2 Effect of Depth of Cut on Cutting Forces

Depth of cut is a fundamental parameter in ball end milling that significantly affects the cutting forces and overall machining efficiency. The cutting forces generated during milling are directly related to the engagement of the cutting tool with the workpiece. Understanding how the depth of cut impacts these aspects is essential for optimizing the milling process, improving productivity, and ensuring the quality of the machined parts. This section examines the impact of depth of cut on the cutting forces and compare with the previous depth of cut and drawing comparisons between them. To analyse the effect of depth of cut, a series of test were conducted keeping another cutting parameter constant. Table 4.2 show the test cutting condition for cutting force analysis.

Test 4	**Test 5**	**Test 6**
D = 300 μm	D = 300 μm	D = 300 μm
$s_t = \frac{2\mu m}{\text{tooth} - \text{rev}}$	$s_t = \frac{2\mu m}{\text{tooth} - \text{rev}}$	$s_t = \frac{2\mu m}{\text{tooth} - \text{rev}}$
N = 2	N = 2	N = 2
z = 10 μm	z = 20 μm	z = 30 μm
n =15000 rpm	n =15000 rpm	n =15000 rpm

Table 4.2 Depth of cut test cutting condition for force analysis

For the test 4, cutting force variation during machining is shown in fig. 4.6. From the figure it can be observed that load is periodical in x, y, z direction. The maximum value of force in x direction is 0.47 N and minimum is -1.5 N. In y- direction the maximum value of load is 1.7 N and minimum is -0.25 N and in z- direction the maximum value off load is 0 N and minimum is -1.8 N.

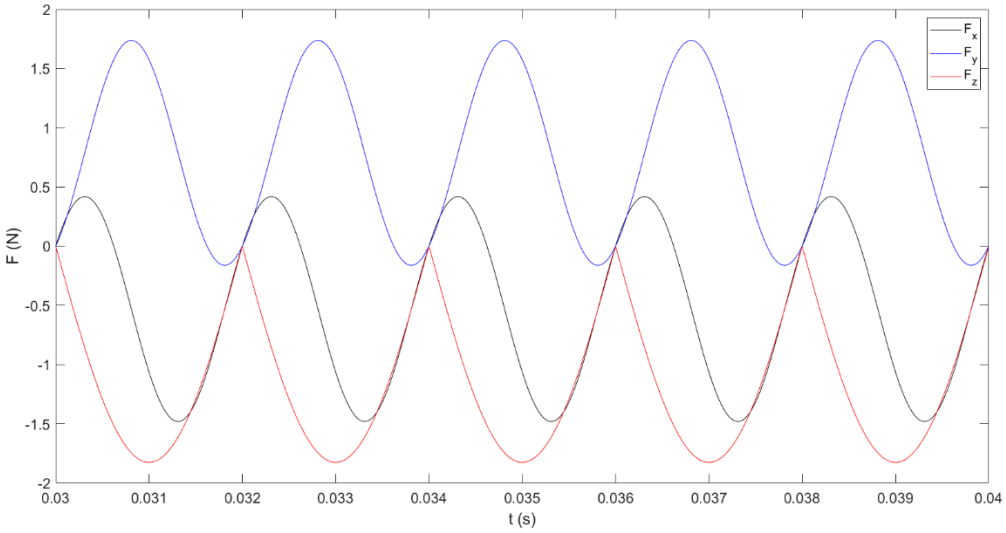

Fig. 4.6 Cutting forces variation for test 4

For the test 5, cutting force variation during machining is shown in fig. 4.7. From the figure it can be observed that load is periodical in x, y, z direction. The maximum value of force in x direction is 0.9 N and minimum is -2.35 N. In y- direction the maximum value of load is 3.4 N and minimum is -0.25 N and in z- direction the maximum value off load is 0 N and minimum is -3.85 N.

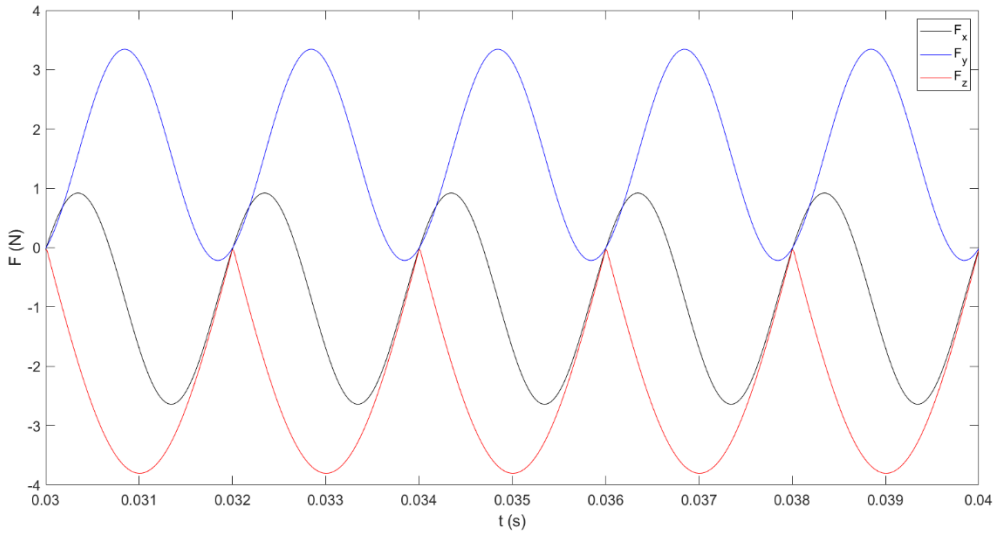

Fig. 4.7 Cutting forces variation for test 5

For the test 6, cutting force variation during machining is shown in fig. 4.8. From the figure it can be observed that load is periodical in x, y, z direction. The maximum value of force in x direction is 1.55 N and minimum is -2.7 N. In y- direction the maximum value of load is 4.3 N and minimum is -0.15 N and in z- direction the maximum value off load is 0 N and minimum is -5.6 N.

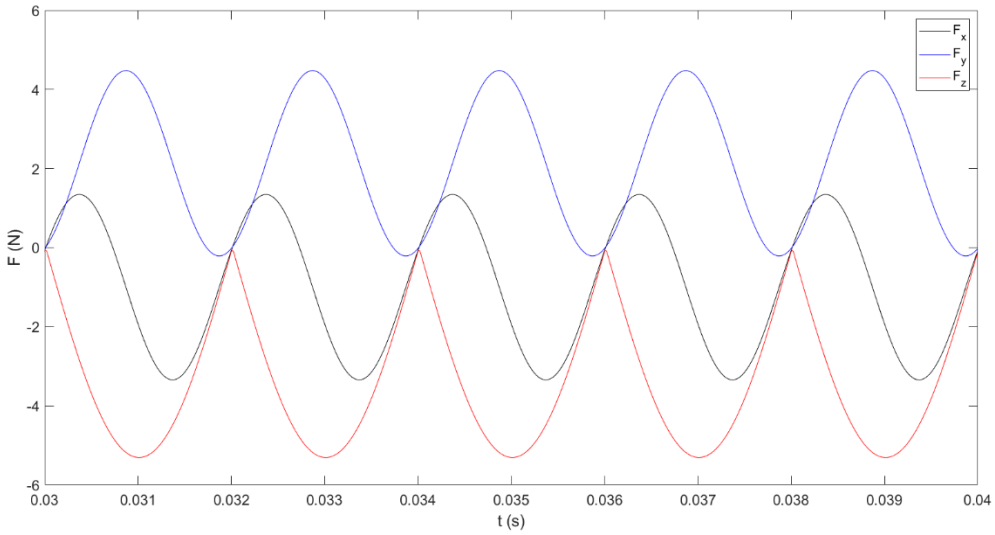

Fig. 4.8 Cutting forces variation for test 6

Testing of the force variation over a wide range of depth of cut conditions is analysed in ball end micro milling. Test are for the slot cutting condition. The results show a clear correlation between the depth of cut and the cutting forces. As the depth of cut increases, the cutting forces in all three directions increase as well. As the depth of cut increases, a larger portion of the tool's cutting edge comes into contact with the material, resulting in higher cutting forces. The cutting forces generated during milling are directly related to the engagement of the cutting tool with the workpiece. Hence, depth of cut is a parameter in ball end milling that significantly affects the cutting forces. These forces act in various directions and can significantly affect the tool's performance and the final surface quality of the machined part. Therefore, it is crucial to have a precise understanding of the relationship between depth of cut and cutting forces to optimize the milling parameters and achieve the desired balance between material removal rate and machining stability.

4.3 Stability Analysis

Stability lobe diagrams graphically represent the relationship between spindle speed and depth of cut, delineating stable and unstable cutting regions. The SLD helps identify the combinations of these parameters that ensure stable cutting conditions, thereby preventing chatter. The SLDs are constructed based on the dynamics of the milling system, including the tool, spindle, and workpiece, and incorporate the effects of cutting parameters and system dynamics. Fig. 4.9 shows the stability lobe diagram (SLD) for ball end micro milling.

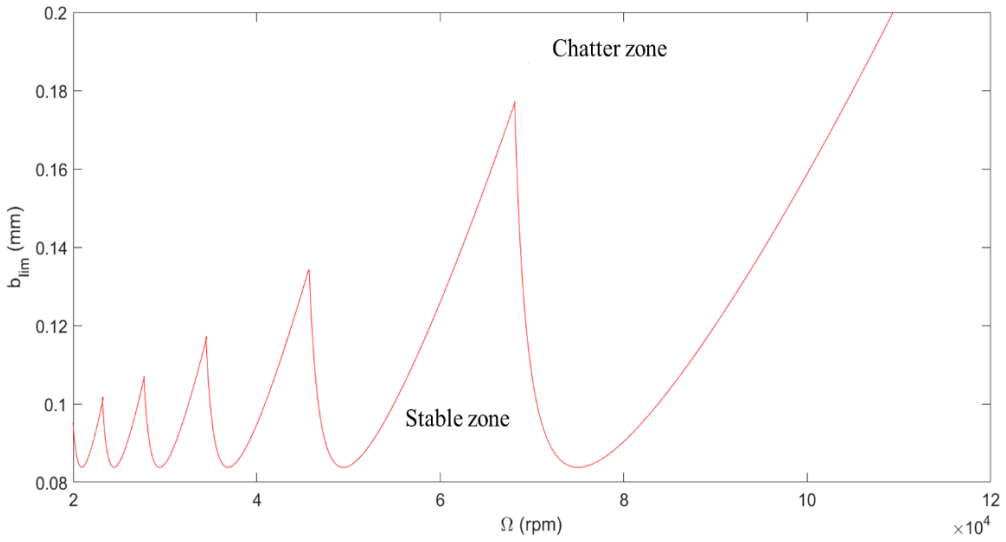

Fig.4.9 Stability lobe diagram for ball end micro milling

It can be clearly seen that the maximum limiting depth of cut is 0.18 mm at 63000 rpm but nearly 75000 rpm its show minimum limiting depth of cut is 0.085 mm. Nearly, 20000 rpm to 38000 rpm its show the median limiting depth of cut in range 0.08 mm to 0.12 mm. But nearly spindle speed 45000 rpm it gives limiting depth of cut 0.138 mm. By using the SLD, practitioners can make informed decisions about spindle speed and depth of cut to maintain stable machining conditions. Thes research provided actionable insights for optimizing milling parameters to prevent chatter, improve surface finish, and extend tool life.

CHAPTER 5

CONCLUSION AND FUTURE SCOPES

This thesis presents a detailed study on chatter modelling for ball end micro milling, with a focus on understanding and predicting the cutting forces and chatter stability. It has been observed that the machining stability is indeed affected by the cutting forces and system dynamics. A comprehensive chatter model was developed, incorporating the dynamic characteristics of the ball end micro milling system. The model was based on the principles of regenerative chatter and included the effects of cutting parameters such as spindle speed, feed rate, and depth of cut. The cutting force model accurately predicted the forces in the X, Y, and Z directions under various cutting conditions. The influence of feed rate and depth of cut on cutting forces was systematically investigated. The construction and application of the Stability Lobe Diagram (SLD) were explored. The SLD effectively mapped the stable and unstable regions for different combinations of spindle speed and depth of cut. From the study following conclusion has been drawn;

- Feed rate and depth of cut affects the cutting forces in ball end micro machining operation.
- With higher feed rates and greater depths of cut leading to increased forces.

- Regenerative chatter affects the surface integrity and tool life. For stable cutting, spindle speed range 55000-65000 gives the optimum cutting condition.

Future Scope

This work can potentially be extended in future to include the following issues:

- Experimental validation under actual cutting conditions and machine tool configurations, would help in refining the model and ensuring its practical relevance and robustness.
- Continued research into optimizing cutting parameters, such as speed, feed, and depth of cut, to achieve better efficiency and surface quality.
- Research and development of new materials and coatings for ball end milling tools to enhance their wear resistance, heat resistance, and overall performance. This can lead to longer tool life and improved machining efficiency.
- Understanding the detailed influence of edge radius on the cutting force and stability lobes for designing tools that are less susceptible to chatter.

References

[1] N. Chen *et al.*, "Advances in micro milling: From tool fabrication to process outcomes," *Int. J. Mach. Tools Manuf.*, vol. 160, no. July 2020, p. 103670, 2021, doi: 10.1016/j.ijmachtools.2020.103670.

[2] Q. BAI, P. WANG, K. CHENG, L. ZHAO, and Y. ZHANG, "Machining dynamics and chatters in micro-milling: A critical review on the state-of-the-art and future perspectives," *Chinese J. Aeronaut.*, 2024, doi: 10.1016/j.cja.2024.02.022.

[3] L. O'Toole, C. W. Kang, and F. Z. Fang, "Precision micro-milling process: state of the art," *Adv. Manuf.*, vol. 9, no. 2, pp. 173–205, 2021, doi: 10.1007/s40436-020-00323-0.

[4] Y. Altinta and P. Lee, "Mechanics and dynamics of ball end milling," *J. Manuf. Sci. Eng. Trans. ASME*, vol. 120, no. 4, pp. 684–692, 1998, doi: 10.1115/1.2830207.

[5] J. Chae, S. S. Park, and T. Freiheit, "Investigation of micro-cutting operations," *Int. J. Mach. Tools Manuf.*, vol. 46, no. 3–4, pp. 313–332, 2006, doi: 10.1016/j.ijmachtools.2005.05.015.

[6] H. Jenkins, *Manufacturing Automation*. 2004. doi: 10.1201/9781420039733.ch26.

[7] G. Quintana and J. Ciurana, "Chatter in machining processes: A review," *Int. J. Mach. Tools Manuf.*, vol. 51, no. 5, pp. 363–376, 2011, doi: 10.1016/j.ijmachtools.2011.01.001.

[8] M. Wiercigroch and A. M. Krivtsov, "Frictional chatter in orthogonal metal cutting," *Philos. Trans. R. Soc. A Math. Phys. Eng. Sci.*, vol. 359, no. 1781, pp. 713–738, 2001, doi: 10.1098/rsta.2000.0752.

[9] M. Wiercigroch and E. Budak, "Sources of nonlinearities, chatter generation and suppression in metal cutting," *Philos. Trans. R. Soc. A Math. Phys. Eng. Sci.*, vol. 359, no. 1781, pp. 663–693, 2001, doi: 10.1098/rsta.2000.0750.

[10] D. Stephenson and J. Agapiou, "Machining Dynamics," *Met. Cut. Theory Pract. Third Ed.*, pp. 665–750, 2016, doi: 10.1201/b19559-13.

[11] R. Faassen, *Chatter Prediction and Control for High-Speed Milling : Modelling and Experiments*. 2007. [Online]. Available: http://wfwweb.wfw.wtb.tue.nl/pdfs/Faassen Ronald.pdf

[12] D. Biermann and A. Baschin, "Influence of cutting edge geometry and cutting edge radius on the stability of micromilling processes," *Prod. Eng.*, vol. 3, no. 4–5, pp. 375–380, 2009, doi: 10.1007/s11740-009-0188-7.

[13] C. Bandapalli, K. K. Singh, B. M. Sutaria, and D. V. Bhatt, "Experimental investigation of machinability parameters in high-speed micro-end milling of titanium (grade-2)," *Int. J. Adv. Manuf. Technol.*, vol. 85, no. 9–12, pp. 2139–2153, 2016, doi: 10.1007/s00170-015-7443-1.

[14] M. Ahmadi, Y. Karpat, O. Acar, and Y. E. Kalay, "Microstructure effects on process outputs in micro scale milling of heat treated Ti6Al4V titanium alloys," *J. Mater.*

Process. Technol., vol. 252, no. July 2017, pp. 333–347, 2018, doi: 10.1016/j.jmatprotec.2017.09.042.

[15] R. Mittal, C. Maheshwari, S. S. Kulkarni, and R. Singh, "Effect of progressive tool wear on the evolution of the dynamic stability limits in high-speed micromilling of Ti-6Al-4V," *J. Manuf. Sci. Eng. Trans. ASME*, vol. 141, no. 10, pp. 1–10, 2019, doi: 10.1115/1.4044713.

[16] M. Yang and H. Park, "The prediction of cutting force in ball-end milling," *Int. J. Mach. Tools Manuf.*, vol. 31, no. 1, pp. 45–54, 1991, doi: 10.1016/0890-6955(91)90050-D.

[17] G. Yücesan and Y. Altmta, "Prediction of ball end milling forces," *J. Manuf. Sci. Eng. Trans. ASME*, vol. 118, no. 1, pp. 95–103, 1996, doi: 10.1115/1.2803652.

[18] S. Wojciechowski and P. Twardowski, "The influence of tool wear on the vibrations during ball end milling of hardened steel," *Procedia CIRP*, vol. 14, pp. 587–592, 2014, doi: 10.1016/j.procir.2014.03.108.

[19] H. A. Sonawane and S. S. Joshi, "Analytical modeling of chip geometry in high-speed ball-end milling on inclined Inconel-718 workpieces," *J. Manuf. Sci. Eng. Trans. ASME*, vol. 137, no. 1, pp. 1–12, 2015, doi: 10.1115/1.4028635.

[20] Z. Peng *et al.*, "Simulation and experimental study on 3D surface topography in micro-ball-end milling," *Int. J. Adv. Manuf. Technol.*, vol. 96, no. 5–8, pp. 1943–1958, 2018, doi: 10.1007/s00170-018-1597-6.

[21] "An Analysis of the Milling Process," vol. 83, pp. 991–992, 1941.

[22] A. C. Ramos, H. Autenrieth, T. Strauß, M. Deuchert, J. Hoffmeister, and V. Schulze, "Characterization of the transition from ploughing to cutting in micro machining and evaluation of the minimum thickness of cut," *J. Mater. Process. Technol.*, vol. 212, no. 3, pp. 594–600, 2012, doi: 10.1016/j.jmatprotec.2011.07.007.

[23] Y. Altintas, G. Stepan, D. Merdol, and Z. Dombovari, "Chatter stability of milling in frequency and discrete time domain," *CIRP J. Manuf. Sci. Technol.*, vol. 1, no. 1, pp. 35–44, 2008, doi: 10.1016/j.cirpj.2008.06.003.